Island Arc (2007) **16,** 575–597

Research Article

Protolith natures and U-Pb sensitive high mass-resolution ion microprobe (SHRIMP) zircon ages of the metabasites in Hainan Island, South China: Implications for geodynamic evolution since the late Precambrian

De-Ru Xu,[1,]* Bin Xia,[1] Peng-Chun Li,[1,2] Guang-Hao Chen,[1] Ci Ma[1,2] and Yu-Quan Zhang[1]

[1]*Key Laboratory of Marginal Sea Geology, Guangzhou Institute of Geochemistry, Chinese Academy of Sciences, Guangzhou 510640, China (email: xuderu@gig.ac.cn), and* [2]*Graduate College of Chinese Academy of Sciences, Beijing 100049, China*

Abstract Metabasites within the Paleozoic volcanic-clastic sedimentary sequences in Hainan Island, South China, show large differences not only in the nature of protoliths, but also in zircon U-Pb sensitive high mass-resolution ion microprobe (SHRIMP) ages. The protoliths for the Tunchang area metabasites have intraoceanic arc geochemical affinities. In the east-central island gabbroic to diabasic rocks and pillow lavas are also present, while the Bangxi area metabasites with back-arc geochemical affinities in the northwest island consist of basaltic, gabbroic and/or picritic rocks. Three types of zircon domains/crystals in the Tunchang area metabasites are defined. Type 1 is comagmatic and yields concordant to approximately concordant 206 Pb/238 U ages ranging from 442.1 ± 13.7 Ma to 514.3 ± 30.2 Ma with a weighted U-Pb mean age of 445 ± 10 Ma. Type 2 is inherited and yields a weighted 207 Pb/206 Pb mean age of 2488.1 ± 8.3 Ma. Type 3 is magmatic with a 207 Pb/206 Pb age of *ca* 1450 Ma. Magmatic zircons in the Bangxi area metabasites yield a weighted U-Pb mean age of 269 ± 4 Ma. We suggest 450 Ma is the minimum age for crystallization of protoliths of the Tunchang area metabasites, because the age range of *ca* 440–514 Ma probably corresponds to both the time of igneous crystallization and the high-temperature overprint. The presence of abundant inherited zircons strongly favors derivation of these rocks from a NMORB-like mantle proximal to continental crust. A protolith age of *ca* 270 Ma for the Bangxi area metabasites probably records expansion of an epircontinental back-arc basin and subsequent generation of a small oceanic basin. The presence of ophiolitic rocks with an age of *ca* 450 Ma, not only in Hainan Island, but also in the Yangtze block, highlights the fact that the South China Caledonian Orogeny was not intracontinental in nature, but characterized by an ocean-related event.

Key words: Gondwana, Hainan Island, intraoceanic subduction, metabasite, Paleo-Tethys, SHRIMP U-Pb dating on zircon, South China.

INTRODUCTION

Multidisciplinary studies on ophiolitic, mafic/ultramafic rock associations in South China (i.e. the amalgamated Yangtze and Cathaysian blocks) reflect that the geodynamic evolution of South China was related to at least two oceans since the Proterozoic: (i) the Paleo-South China ocean, located between the Cathaysian and the Yangtze blocks, probably opening from the Mesoproterozoic onward (Guo *et al.* 1985, 1996; Chen *et al.* 1991), and (ii) the Paleo-Tethys, surrounding the South China and probably opening from the early Carboniferous onward (Zhang *et al.* 1994; Metcalfe 1996, 2000; Liu *et al.* 2005 and references therein).

*Correspondence.

Received 16 June 2006; accepted for publication 13 May 2007.

doi:10.1111/j.1440-1738.2007.00584.x

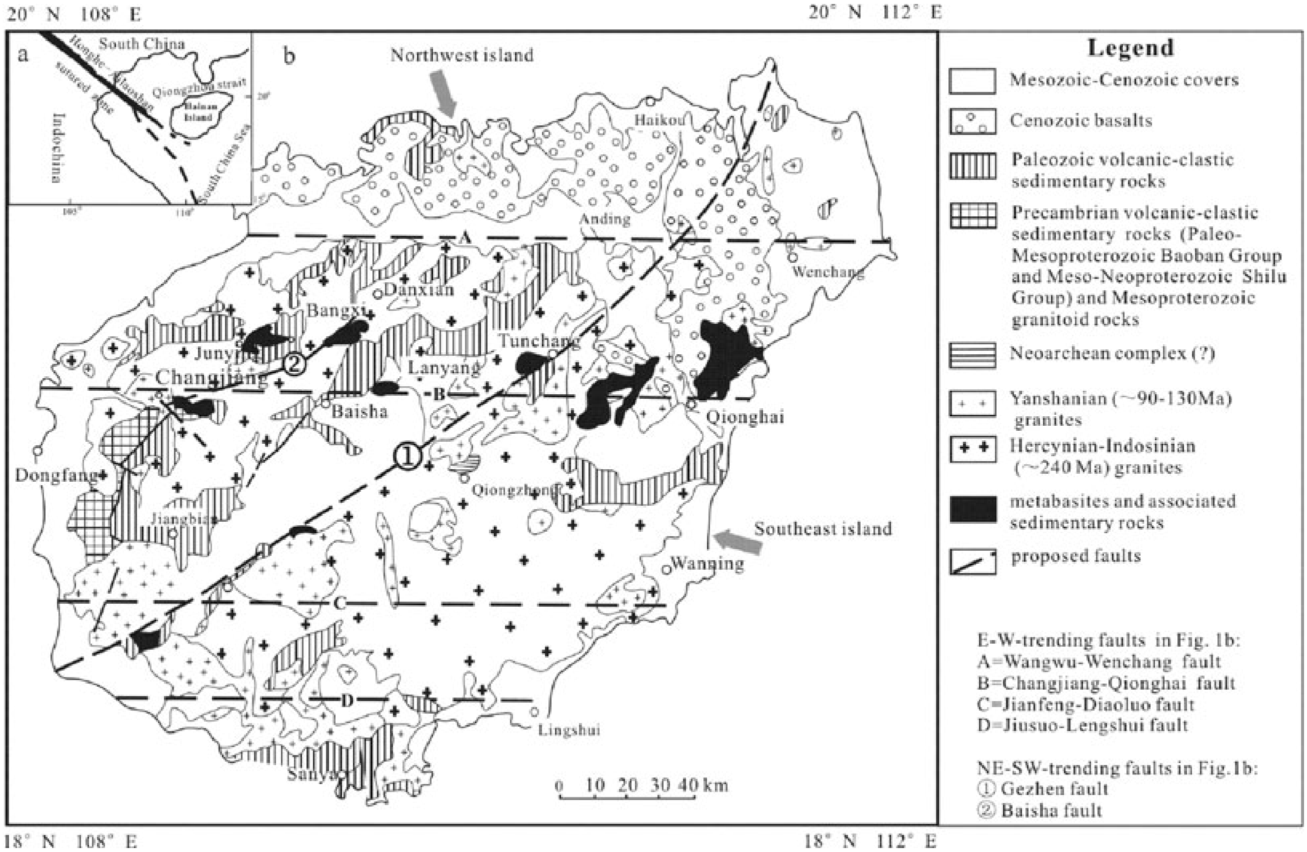

Fig. 1 Simplified geological map of Hainan Island, China, showing the main tectono-stratigraphic and tectono-magmatic units. Note: tectono-stratigraphic subdivision of Hainan Island into the southeast and the northwest islands after Metcalfe *et al.* (1993).

The closure of these oceans in response to convergences between the Yangtze and the Cathaysian, between the South China and the Indochina, and between the South China and the North China blocks, eventually resulted in the present South China, characterized by a high complexity of nappe structures (e.g. Hsü *et al.* 1988, 1990; Yan *et al.* 2003). In order to unravel the preorogenic paleogeography and the complex tectono-magmatic-metamorphic processes of the South China, a series of different models involving the Proterozoic trench-arc-back arc basin system (Guo *et al.* 1985, 1996), the Rodinia breakup leading to the late Neoproterozoic Nanhua trough (Li *et al.* 1999, 2003) and the Mesozoic continent-continent collision (Hsü *et al.* 1988, 1990), have been suggested for the evolutionary history of South China over the many years of geological research. However, the interpretation of South China is still a matter of debate, because whether the observed mafic/ultramafic rocks veritably represent remnants of oceanic crusts, and if so, when the magmatic crystallization of these ophiolitic rocks took place, have not been well constrained (Wu 2003 and references therin).

Hainan Island in China, separated from the Cathaysian block of South China by the Qiongzhou strait (Fig. 1a), is a continental-type island. Abundant metabasites within the Paleozoic volcanic-clastic sedimentary sequences occur widely in this Island (Fig. 1b). The geochemical and isotopic data appear to favor an interpretation of these metabasites as relics of fragmented oceanic crust of the eastern part of Paleo-Tethys (e.g. Li *et al.* 2002). Available geochemical and Sr-Nd isotopic results, however, show that the Tunchang area metabasites in the east-central island might have been generated above an intraoceanic arc or supra-subduction zone-like setting, whereas the Bangxi area metabasites in the northwest island more likely represent the expansion of a marginal basin (epircontinental back-arc basin) followed by the generation of a young oceanic crust (Xu *et al.* 2007; in review). Because the ages, the rock associations and the protolith natures of these metabasites have not been well constrained, the suggested tectonic settings for these rocks still are ambiguous. As a result, previously geological, petrographic and geochemical data constrained a late Paleozoic intracontinental magmatism for these metabasites, owing to lithosphere thinning (Xia *et al*. 1991a,b; Fang *et al*. 1992). Despite the lacks of typical spinifex textures and the arguable dating by whole rock Sm-Nd methods, an interpretation of these metabasites as the Proterozoic komatitic basalts also was proposed by Zhang *et al*. (1998) and Liang *et al*. (2000). Obviously, detailed studies on the protolith natures and ages of the metabasites in Hainan Island are still needed, and also of extremely importance, to identify the existences of some oceans at the times, as inferred from the previously suggested suture zones (e.g. Yang *et al*. 1989; Hsü *et al*. 1990; Metcalfe *et al*. 1993; Chen *et al*. 1994; Li *et al*. 2002). These in turn allow a greater understanding of what these rocks can tell us about the tectonic processes as well as the formation and evolution of Hainan Island, with respect to the tectonic evolution of South China.

Based on new geological and petrographical investigation, in this paper, a Cathodoluminescence (CL)-controlled sensitive high mass-resolution ion microprobe (SHRIMP) U-Pb dating on zircon has been carried out, in order to (i) determine the ages of the protoliths of metabasites both in the Tunchang and the Bangxi areas, and (ii) better understand their representative tectono-magmatic-metamorphic events. Our studied results confirm that the metabasites within the Paleozoic volcanic-clastic sedimentary sequences in Hainan Island, South China, were diachronous and probably recorded two stages of oceanization.

REGIONAL GEOLOGY

The strata cropped out in Hainan Island include Paleozoic-dominated, Proterozoic, Paleozoic, Mesozoic and Cenozoic. The Precambrian rocks (Fig. 1b), composed of the underlying Mesoproterozoic Baoban Group (*ca* 1800–1400 Ma) and the overlying Meso-Neoproterozoic Shilu Group (*ca* 800–1100 Ma), have been reinterpreted as basement to the Island (Wang *et al*. 1991). An older basement probably underlying the Island also can be inferred from that the gneissic charnockite-amphibolite assemblages in Qiongzhong, the east-central island have a zircon U-Pb age of *ca* 2560 Ma (Zhang *et al*. 1997a).

The Shilu Group comprising of iron-rich metavolcanic-clastic sediments with typically turbidite sequence has been defined only in the northwest island (Fig. 1b). This Group is overlain unconformably by Sinian to Silurian (?) neritic facies volcanic-clastics and in turn overlain unconformably by Carboniferous basal conglomerates followed by meta-shales, quartzites, conglomerates and diamictites. The Carboniferous rocks are conformably covered by the Lower Permian rocks, which the latter contains fusulinid foraminifera and is unconformably overlain by the Cretaceous continental siltstones and mudstones. Locally, the Upper Lower Triassic mudstones overly the Carboniferous in a few small isolated grabens and then are overlain uncomformably by the Cretaceous rocks. The Cretaceous rocks are further overlain by the Mid-Eocene red mudstones and carbonaceous shales, and then by basalts of Neogene and Quaternary ages. In the southeast island, the Lower to Middle Cambrian and Ordovician rocks in Shanya area (Fig. 1b) are composed of manganese- and phosphorite-bearing carbonates with trilobite fossils, stromatolitic limestones, calcareous argillites, siltstones and quartzites. These early Paleozoic sequences are underlain unconformably by the Carboniferous rocks, and then directly covered by the Cretaceous rocks.

The major structural patterns (i.e. faults and folds) in the Island show an east–west and northeast–southwest orientation. The east–west structures are dominated by four faults: the Wangwu-Wenjiao fault, the Changjiang-Qionghai fault, the Jianfeng-Diaoluo fault and the Jiusuo-Lengshui fault, from the north to the south (Fig. 1b). The northeast–southwest structures consist of a few short-axis uplifts and depressions, which are controlled by a series of marginal faults, e.g. the northeast–southwest trending-Baisha and Gezhen faults, respectively, in the East-central and the north-west Islands. All these faults began with their activities probably at Proterozoic, or Early Paleozoic, or Late Paleozoic and/or Mesozoic (Wang *et al*. 1991).

Polyphase intrusive and extrusive rocks are widespread in the Island. The Hercynian to Indosinian syncollisional S-type granites (*ca* 240 Ma of SHRIMP zircon U-Pb age: Li *et al*. 2005), and Yanshanian granites (*ca* 90–130 Ma: Wang *et al*. 1991) are major intrusions and take up 60% area of the Island (Fig. 1b). Because of the complicated tectonism and polyphase magmatism, all the pre-Paleozoic rocks in the Island generally have a greenschist to upper amphibolite facies and/or up to eclogite facies metamorphism (Xia *et al*. 1991a,b; Wang *et al*. 1991; Xu *et al*. 2006).

FIELD DESCRIPTION AND PETROGRAPHY

This paper focuses on the metabasites, respectively, in Tunchang area, the east-central island, and Bangxi area, the northwest island (Fig. 1b). Because of extremely poor outcrop resulting from the thick Quaternary cover sequence and heavy forest cover, the detailed field description and petrography of the Tunchang area metabasites have been done in this study, whereas the geological and petrographical data of the Bangxi area metabasites are cited mainly from Xia *et al.* (1991a,b), Fang *et al.* (1992) and Zhang *et al.* (1998).

THE TUNCHANG AREA METABASITES

The Tunchang area metabasites in the east-central island are situated at the region between the Yashiyuan and the Xichangyuan with longitude and latitude ranging from 109°57′ 22″ to 109°58′ 15″ and from 19°25′ 30″ to 19°26′ 15″, respectively (Fig. 2). Our field investigations indicate that the rocks outcropping in this area are rather complex. The metabasite body itself shows a wedge-shape with a northeast-trending axis and has a length of about 3.0 km and a width of about 0.6 km. The main foliation within the body trends NNE-NNW dipping east at an angle of *ca* 50–70° (Fig. 2a). There is an associated roughly shive-parallel mineral lineation. The Carboniferous (?) host rocks comprise of a set of huge thick, low-grade argillaceous, arenaceous and silicious sediments of middle-deep marine facies origin. Two metamorphic zones, i.e. the sericite and the biotite, have been identified in this area (Fig. 2a), based on the first appearance of biotite. The biotite zone only occurs locally in the western part of the metabasite body and has a width of *ca* 50–200 m. Up to meter-scale tight to isoclinal folds and possible migmatition are also observed in this zone (Fig. 3a). The melanosomes in the zone are composed of biotite and muscovite, with quartz, opaque minerals, apatite, zircon and monazite as accessory phases, whereas the leucosomes are granitic in composition. The similarity in strike and dip to the metabasite body indicate the biotite zone occurs as an interlayer within the metabasites. The sericite zone crops out widely in the studied area and generally exhibits northeast-trending schistosity and stratification, both of which roughly dip W at an angle of 35–70°. Fault contacts in the northwest and the southeast mark the boundaries between the sericite zone and the metabasite body (Fig. 2a), while the Yanshanian granites intruded into the host rocks.

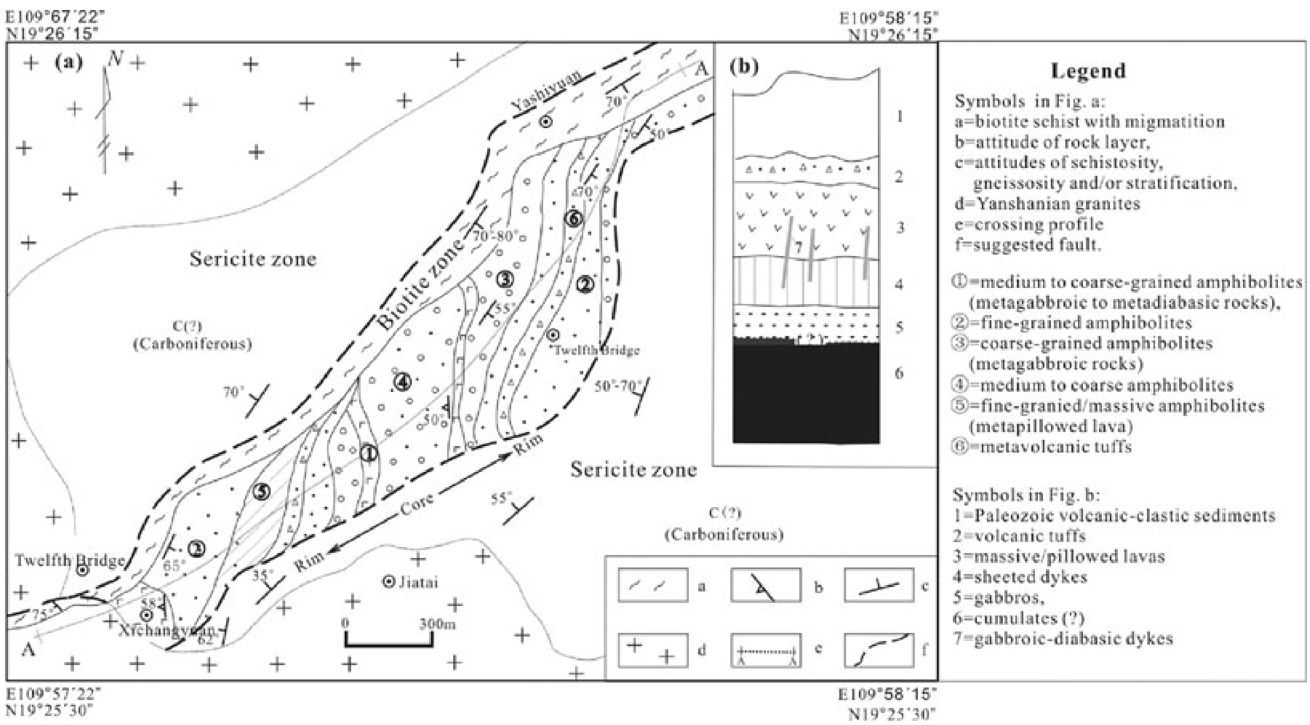

Fig. 2 Geological map shows the metabasite complex in Tunchang (i.e. Chenxing) area, the east-central Hainan Island (a) and the possible Ophiolitic unit (b). Note: these metabasites are generally fine-grained near the margins, and become coarse-grained towards the cores, which are cross-cut by diabasic-gabbroic dykes, probably indicating an incomplete, dismembered ophiolitic suite.

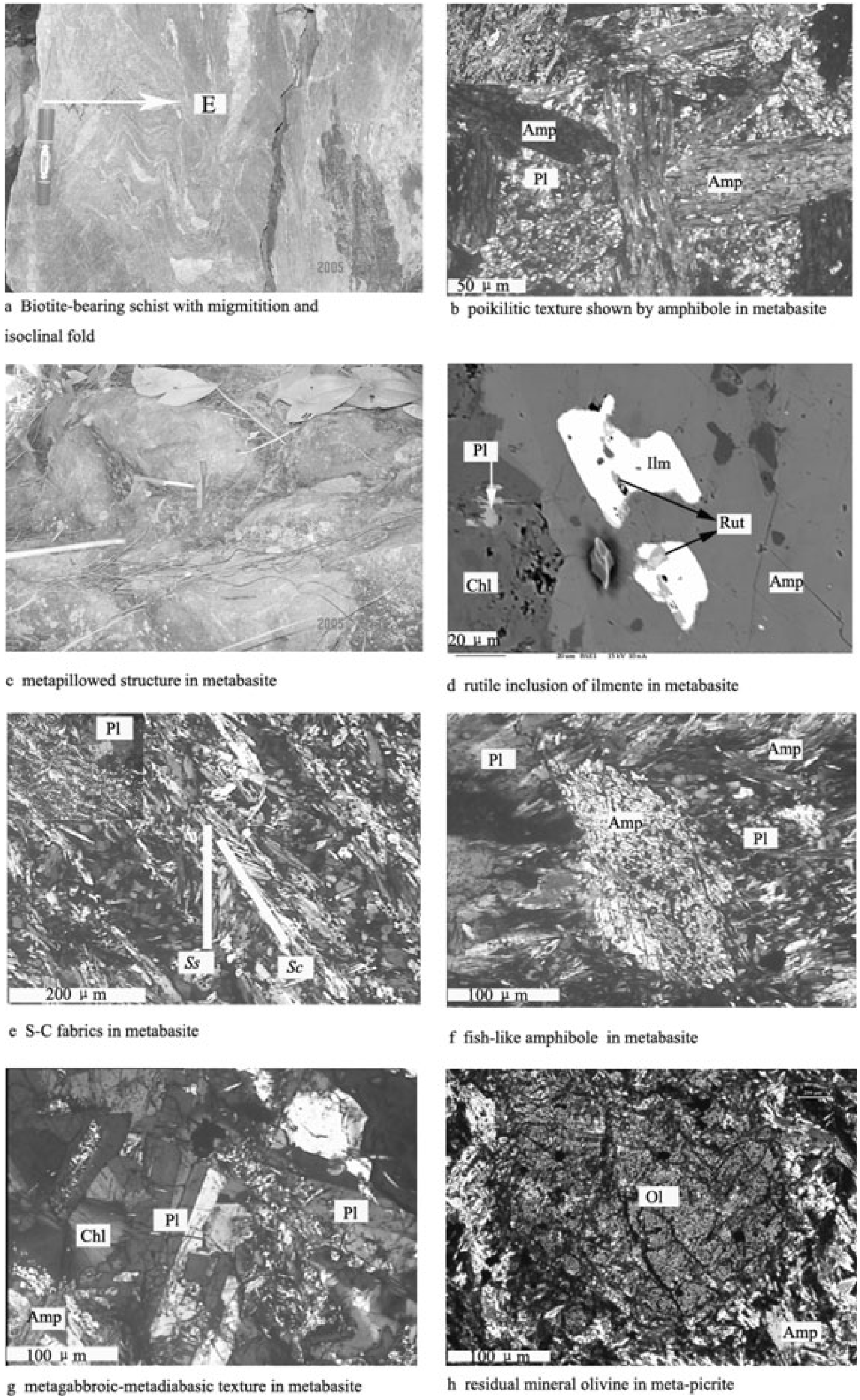

Fig. 3 Field photograph and thin-section photomicrograph of the metabasites and associated host rocks in Tunchang area, the east-central island (a–f) and Bangxi area, the northwest island (h), respectively. Red pen and hammer, respectively, in field photographs (a) and (f) showing the sizes. Figure 4d is BSE image and others are cross-polarized light photomicrographs. Amp, amphibole; Chl, chlorite; Ilm, ilmenite; Ol, olivine; Pl, plagioclase; Rut, rutile.

The rock assemblages of the Tunchang area metabasites comprise of coarse-grained, medium to fine-grained and massive/or fine-grained amphibolites, and then are crosscut by medium to coarse-grained amphibolites. These rocks appear to be fine-grained near the margin, and become coarse-grained towards the core (Fig. 2a). The coarse-grained amphibolites are dark and dark-green in color, and contain radiating clusters of green, cylindrical amphibole with a length of 0.5–3 cm, and milky, porphyritic plagioclase with a size of about 0.5–1 cm. These rocks often have a homogeneous, poikilitic texture shown by pseudomorphic amphiboles after pyroxenes (Fig. 3b), and thus most of their primary rocks are proposed to be cumulus, gabbroic rocks. The medium to fine-grained, massive/or fine-grained but more foliated texture amphibolites of green-gray to green color are equigranular and have the same mineral assemblage as their coarse-grained equivalents. The relics of pillowed structures are well preserved in these rocks (Fig. 3c). Rare metavolcanic tuff covers the underlying meta-pillow lava. Locally, massive and disseminated sulfide mineralization (mainly pyrite) hosted by massive or fine-grained rocks, is well developed. Ultramafic rocks appear to be missing, but the presence of such rocks at deeper levels cannot be ruled out.

Thin section observations show that magmatic minerals pyroxene, olivine and/or hornblende are no longer preserved in our studied metabasites, and amphibole pseudomorphs after pyroxene and chlorite pseudomorphs after olivine or amphibole can be seen. Besides major minerals of amphibole, plagioclase (dominated by albite and oligoclase-labradorite) and chlorite, Ti minerals are also present in these rocks. Minor rutile grains as idioblastic crystals (*ca* 10 μm) or pods of small crystals may present in ilmenite (Fig. 3d). Minor muscovite, prehnite and tourmaline also occur as secondary minerals.

The Tunchang area metabasites are characterized by intense ductile-brittle shear deformation. Our observations display that these rocks vary from slightly to strongly foliated, and the fine-grained samples generally contain a main foliation defined primarily by olive-green, pleochroic amphibole grains and plagioclase grains, which form either interfingered nets of 1–4 mm diameter or clusters of elongated crystals up to 5 mm in length. Thus the fine-grained samples contain a perfect nematoblastic texture and a well-expressed orientation of minerals along the schistosity (Fig. 3e). The amphibole from the coarser-grained samples does not show a well-expressed mineral orientation, but commonly contains a mylonitic texture with undulose extinction and fish-like shape in a very fine-grained matrix (Fig. 3f). Despite the intense deformation and metamorphism, our studied rocks sometimes preserve gabbroic to diabasic textures in medium to coarse-grained amphibolites (Fig. 3g).

Collectively, the protoliths for the Tunchang area metabasites most likely are coarse-grained gabbroic rocks, medium to fine-grained gabbroic rocks and fine-grained and/or massive pillowed lava, which are intruded by diabasic to gabbroic dykes, and in turn are covered by the volcanic-clastic sediments. These rocks are subjected to intensive deformation and alteration. In connection with the geochemical data (*see the summary, below*), we thus suggest that the Tunchang area metabasites most likely represent the upper layers of an unkown ophiolite or an incomplete, dismembered ophiolite body (Fig. 2b).

THE BANGXI AREA METABASITES

The Bangxi area metabasites have been exposed in the northwest island from Shilu (i.e. Changjiang), Junying via Bangxi to Nanyang along the east–west-trending Changjiang-Qionghai fault zone, by an elongation of about 180 km (Fig. 1b). As discontinuous, lensoid or stratiform-like bodies, these rocks have an east–west strike with the well-developed schistosities dipping to *ca* 205° southwest and are intercalated within the Ordovican metavolcanic-clastics (Fig. 4), which comprise of phyllites, fine-grained sandstones, siltstones, mica-bearing quartz schists, chlorite-bearing quartz schists and locally dolomitic rocks of marine to neritic facies. The host rocks show an overall east–west strike with both to south and north dips, and are intruded by the Hercynian-Indosinian granites, which in turn are intruded by the Yanshanian granites. Because of the rather complex stratigraphic sequences and associated deformation in the Shilu-Junying-Bangxi terrane, Yang *et al.* (1989) and Hsü *et al.* (1990) interpreted this area as a late Paleozoic-early Mesozoic tectonic mélange complex and named it the 'Shilu mélange'.

The Bangxi area metabasites generally display a greenschist facies metamorphism and contain two major lithotypes: coarse-grained with dark to dark-green color and fine-grained with a green-gray color. The coarse-grained rocks with a porphyritic texture are predominant and include minerals of plagioclase and pseudomorphic actinolite after pyroxene (accounting for 85% to 90%); whereas the fine-grained rocks with a nematoblastic texture contain a major mineral albite. In the less altered rocks, igneous textures such as amygdaloid and pillow structures are locally preserved (Zhang *et al.* 1998). The residual magmatic mineral olivine, which is highly cataclastic and surrounded by matrix of amphibole, also has been found in the coarse-grained metabasite sample 05BX04-1 (Fig. 3h). Compositionally (see the summary, below), the Bangxi area metabasites are mafic/ultramafic in nature and thus, the protoliths for these rocks most likely are basaltic rocks

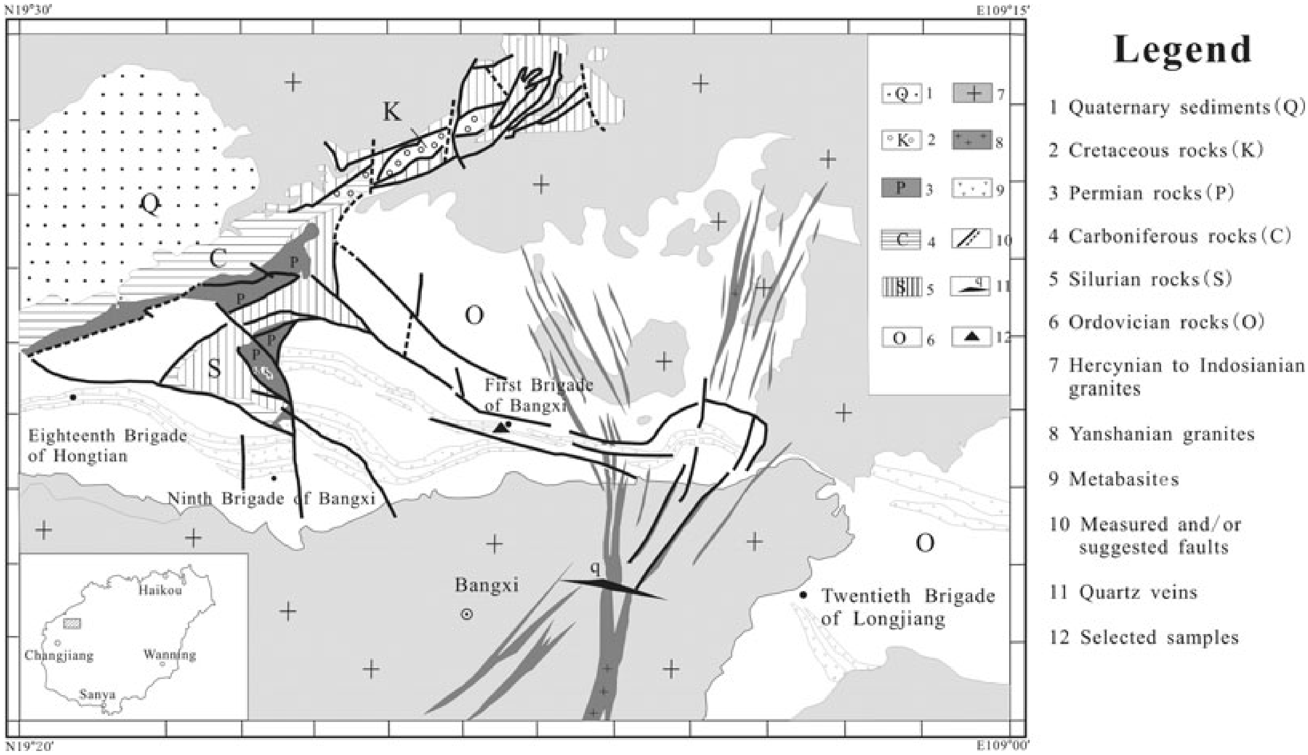

Fig. 4 Sketch map showing regional geology of the Bangxi area metabasites in the northwest island.

(fine-grained), gabbroic and/or picritic rocks (coarse-grained).

SUMMARY ON GEOCHEMISTRY AND Nd ISOTOPE

The geochemical and Nd isotopic data (Xu *et al.* 2001, 2007; Li *et al.* 2002; in review) show that the Tunchang area metbasites in the east-central island typically have an affinity to low-Ti tholeiites with the ratios of Ti/Y < 350 and Zr/Y < 3, and the SiO_2 contents between 44.7 wt% and 55.7 wt%. These rocks generally contain extremely low concentrations in high field strength elements (HFSE) and rare earth elements (REE) (an overall enrichment of 5–12 times chondrite: Sun & McDonough 1989), and are characterized by a strongly light REE (LREE)-depleted pattern ($La/Yb_{cn} = 0.14$–0.53) except for a few boninite-like samples with a concave-up, slightly LREE-enriched pattern (Fig. 5a). The primitive mantle-normalized spidergrams (Fig. 5b) also reveal that these rocks generally are enriched in large ion lithophile elemets (LILE) such as Ba, Rb, Sr and U, and strongly depleted in HFSEs such as Nb, Ti, Y, Zr, Hf and Th, relative to the normal mid-ocean ridge basalts (NMORB) and primitive mantle (Sun & McDonough 1989). The low ratios of Ti/V (6–20) and Ce/Yb (generally < 2.2), the high Mg-number (55–82) and the contents of Zr (8.0–37.0×10^{-6}), Cr (540–3100×10^{-6}) and Ni (160–470×10^{-6}), are indicative of a plume-influenced magma intraoceanic arc source (Teklay *et al.* 2002; Manikyamba *et al.* 2004), being consistent with a high ε_{Nd}(450 Ma: based on this study) value (+3.0 to +6.1). These features imply that the protoliths for the Tunchang area metabasites are relics of an intraoceanic arc, and the parental melts to these rocks were generated from a depleted, primitive mantle arc source rather than an NMORB source in a supra-subduction zone or subduction-related slow-spreading mid-ocean ridge settings (e.g. Robertson 2002).

The Bangxi area metabasites in the northwest island are distinctive in geochemistry and Nd isotope from the Tunchang area metabasites, but are comparable to the Shuanggou ophiolites in the Honghe-Ailaoshan sutured zone, South China (Figs 1a,6). These rocks show high but variable MgO (up to 28.2 wt%), TiO_2 (up to 2.5 wt%) and Na_2O (up to 3.5 wt%) contents, low but variable SiO_2 contents (40.7–54.3 wt%), and high but variable Zr (50–250×10^{-6}), Y (12.50–43.50×10^{-6}), Cr (285–2526×10^{-6}) and Ni (48–1219×10^{-6}) concentrations (cf. Xia *et al.* 1991b; Fang *et al.* 1992; Xu

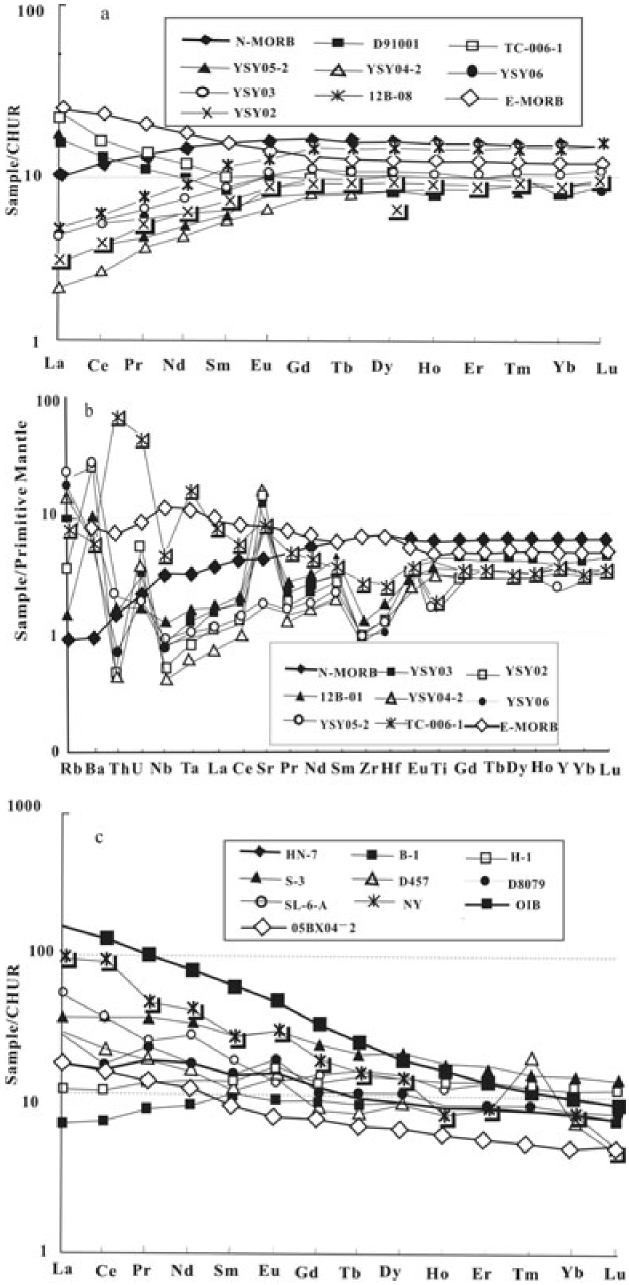

Fig. 5 Chondrite-normalized rare earth element spectra and primitive mantle-normalized multielement plots for the metabasites from both the Tunchang (a,b) and the Bangxi areas (c), respectively. Chondrite rare earth element (REE) compositions, primitive mantle normalization values, NMORB, enriched MORB and oceanic island basalt (OIB) values from Sun and McDonough (1989). Data for the Tunchang area metabasites from Xu *et al.* (2007; in review), whereas data for the Bangxi area metabasites from Xia *et al.* (1991b), Fang *et al.* (1992), Li *et al.* (2002) and this study.

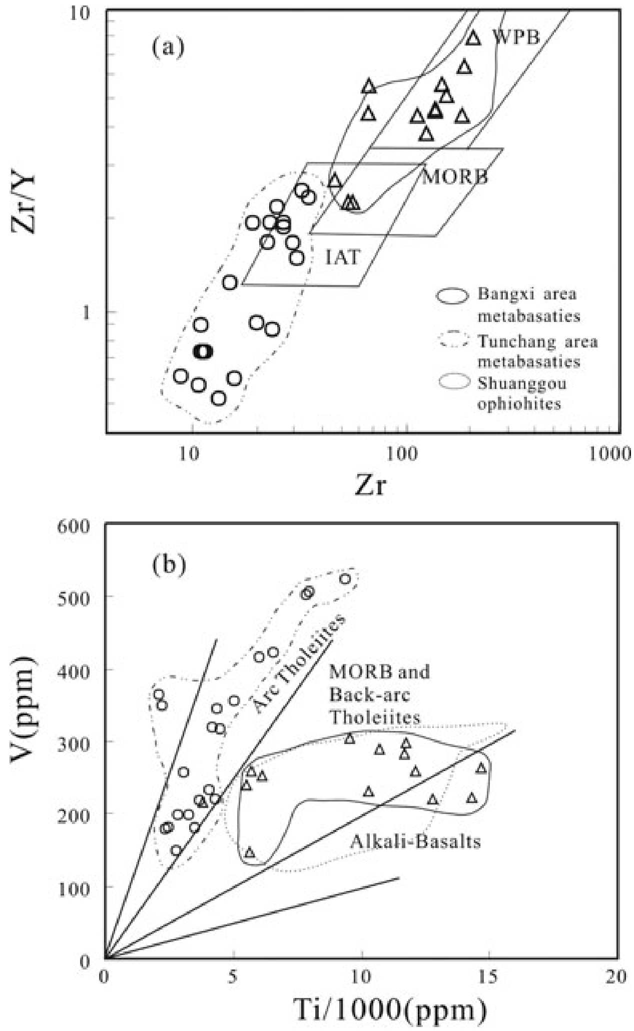

Fig. 6 Plots of Zr *vs* Zr/Y (a) and V *vs* Ti/1000 (b) for the metabasites from both the Tunchang and Bangxi areas, after Pearce and Norry (1979), and Shervais (1982). IAT, island arc basalts; MORB, mid-oceanic ridge basalt; WPB, within plate basalts. The Bangxi area metabasites from Xia *et al.* (1991b), Fang *et al.* (1992), Zhang *et al.* (1998), Xu *et al.* (2001), Li *et al.* (2002) and this study, the Tunchang area metabasites from Li *et al.* (2002) and Xu *et al.* (2007; in review), and the Shuanggou ophiolites from Zhang *et al.* (1994).

et al. 2001; Li *et al.* 2002 and this study). They also occupy high but variable REE concentrations ($24–120 \times 10^{-6}$) and REE patterns dominated by LREE-enriched type with minor occurrence of LREE-depleted type (Fig. 5c). The ε_{Nd} (270 Ma: based on this study) values (–4.4 to +6.8) (cf. Fang *et al.* 1992 and Li *et al.* 2002) suggest a highly depleted to an enriched mantle source for these rocks. Thus the Bangxi area metabasites most likely occurred during the extension of a back-arc basin or marginal basin as a result of the activity of mantle plume (e.g. Jahn 1986). The extension of the basin probably was quick and so that, a small oceanic basin could have been formed at that time, based on geochemical signature (e.g. the occurrence of NMORB-like compositions) and geological observation (e.g. an extrusive feature of submarine facies for these rocks: Xia *et al.* 1991a,b).

SHRIMP ZIRCON U-Pb DATING

SAMPLE SELECTION AND ANALYTICAL METHODS

For the purpose of SHRIMP zircon U-Pb dating, three metabasite samples TC001 (medium to coarse-grained metadiabasic rock), YSY05-2 (coarse-grained metagabbroic rock) and YSY03 (fine/massive metapillowed lava) from the Tunchang area, and one metabasite sample 05BX04-2 (coarse-grained metagrabbroic rock) from the Bangxi area are selected, respectively. Representative zircons are obtained by a standard procedure of crushing, sieving, magnetic and electromagnetic density separation, and hand picking. Zircon samples and transmission electron microscopy (TEM) reference material were mounted onto double-sided adhesive tape and enclosed in an epoxy resin disc. The disc was polished, cleaned and gold-coated (Williams 1992; Song *et al.* 2002). The zircons were examined with reflection and transmitted light and cathodoluminescense (CL) images to reveal their internal structure. The locations of the ion probe measurements were marked on the zircons before analysis (Figs 7–9).

Analyses for U-Pb compositions used the SHRIMP II ion microprobe at Beijing SHRIMP Center, China. The U-Pb ratio of the TEM zircon reference material was corrected using the SL13 standard (age: 572 Ma; U: 238×10^{-6}). Analysis of the reference sample was performed after four analyses of unknown zircons, so the quality of the analyses was closely controlled. The mean $^{206}Pb/^{238}U$ age for 31 analyses of the TEM reference sample was 417 Ma, indistinguishable from the certified value 417 Ma (Black *et al.* 2003). Data processing was carried out using the ISOPLOT programs of Ludwig (Ludwig 1999, 2001). Corrections for common Pb used the measured abundances of ^{204}Pb. The error of a single analytical result shown in Tables 1 and 2 is expressed as 1 standard deviation, 1σ. The final age result used is the weighted mean of $^{206}Pb/^{238}U$ and/or $^{207}Pb/^{206}Pb$ ages and the error is quoted at 2ó. All mean ages are quoted with 95% confidence limits. Our statistic analysis has ruled out those analyzed spots with discordant degree greater than 50% and/or a percentage of common ^{206}Pb greater than 5%.

RESULTS

THE TUNCHANG AREA METABASITES

Fifteen, 12 and 19 zircon crystals were recovered, respectively, from the Tunchang area metabasite samples TC001, YSY05-2 and YSY03. These zircons have a grain size ranging from 60 to 150 μm

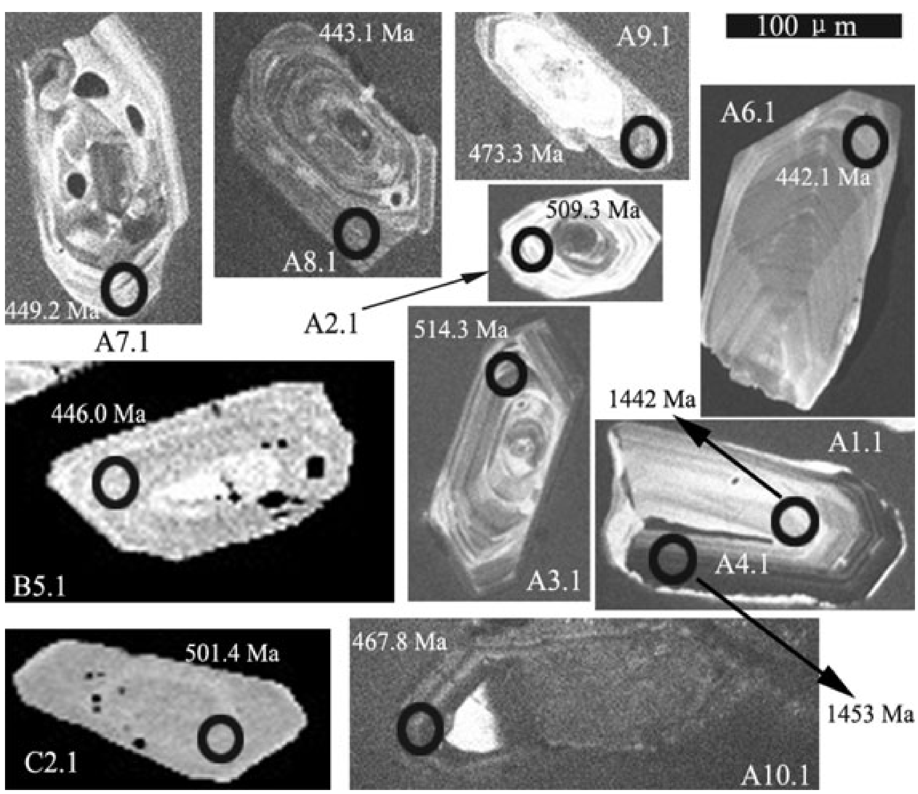

Fig. 7 Cathodoluminescence (CL) images of zircons in the Tunchang area metabasite samples TC001 (A), YSY03 (B) and YSY05-2(C) from the east-central island. A7.1 representing analyzed spot. The ages for spots A1.1 and A4.1 (Type 2) marked in the figure are Pb-Pb data, whereas others (Type 1) are U-Pb data. Note, all zircon domains/crystal are typical comagmatic, but affected due to high temperature overprint.

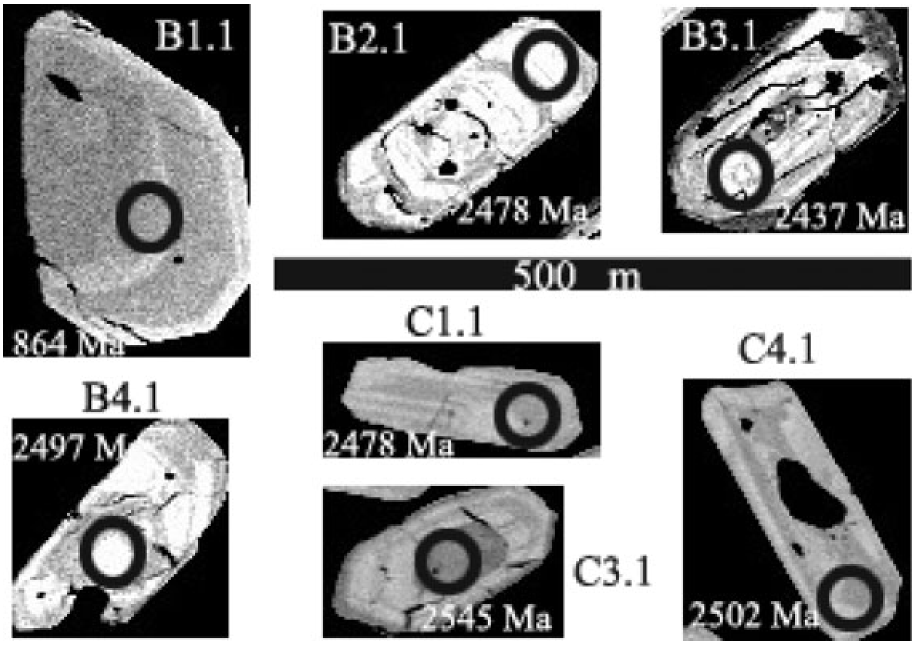

Fig. 8 Cathodoluminescence (CL) images of zircons in the Tunchang area metabasite samples YSY03 (B) and YSY05-2 (C) from the east-central island. B4.1 representing analyzed spot, and all ages marked in the Fig. by Pb-Pb data.

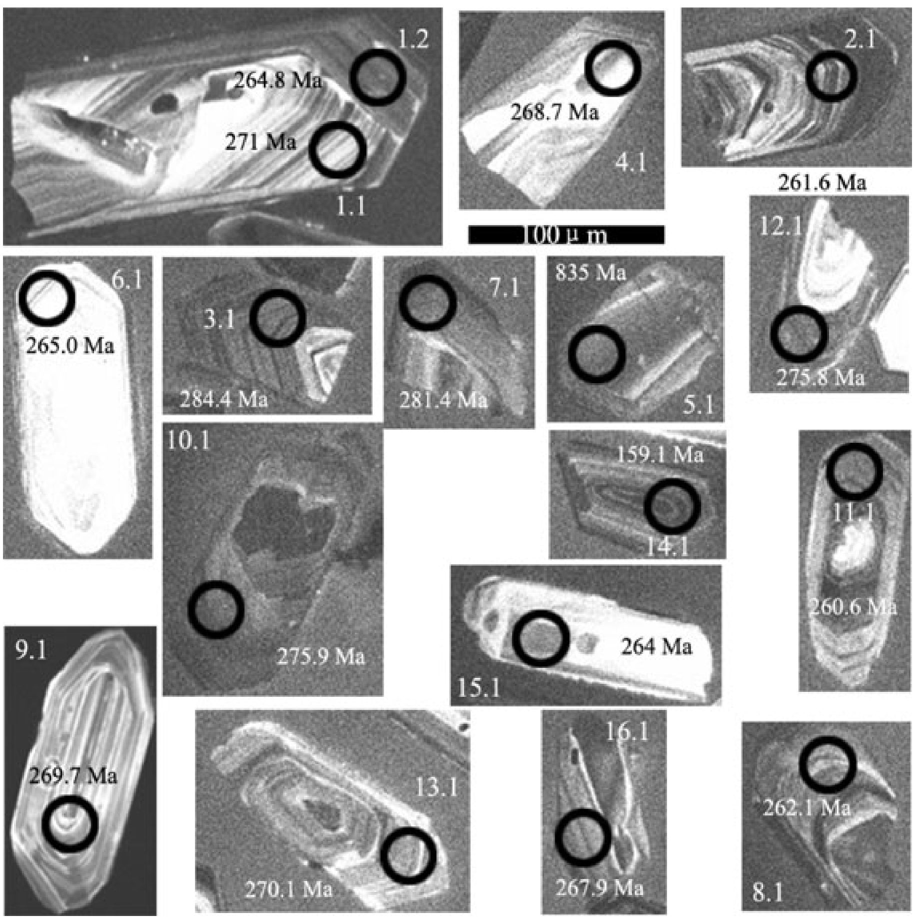

Fig. 9 Cathodoluminescence (CL) images of zircons in the Bangxi area metabasite samples 05BX04-2 from the northwest island. Shown in the figure are zircon U-Pb ages except for the spot 5.1 with a Pb/Pb age of *ca* 835 Ma.

long and 40–120 μm wide. Most of these zircons in the samples are light yellow in color and show more or less euhedral shapes. A few zircons are colorless, transparent, euhedral and prismatic in morphology. CL images show that the internal structures of zircon in the Tunchang area samples are rather complex (Figs 7,8), and three types of zircon domains/zircon crystals have been defined

Table 1 SHRIMP U-Pb data for the Tunchang area metabasite samples TC001(A),YSY03(B) and YSY05-2(C) in the east-central Hainan Island, South China (those with discordant degree out of 50% and/or percentage of common ^{206}Pb more than 5% are not listed in the Table)

Analysed spot	ppm U	ppm Th	$^{232}Th/^{238}U$	ppm $^{206}Pb^*$	*f*206/%	$^{207}Pb/^{206}Pb^*$	±%	$^{207}Pb^*/^{235}U$	±%	$^{206}Pb^*/^{238}U$	±%	t($^{206}Pb/^{238}U$) (Ma)	±%	t($^{207}Pb/^{206}Pb$) (Ma)	±%
A1.1	270	103	0.39	61.5	0.16	0.0908	1.2	3.31	3.2	0.2647	3.0	1513.9	40.4	1442	23
A2.1	267	191	0.74	18.9	0.31	0.0596	3.0	0.68	4.3	0.0822	3.1	509.3	15.4	588	64
A3.1	588	346	0.61	42.0	0.29	0.0558	2.8	0.64	6.7	0.0830	6.1	514.3	30.2	443	61
A4.1	1482	486	0.34	281.2	0.07	0.0913	0.5	2.78	3.0	0.2207	2.9	1285.7	34.1	1453	10
A6.1	120	73	0.63	7.4	1.20	0.0574	6.2	0.56	7.0	0.0710	3.2	442.1	13.7	506	137
A7.1	453	145	0.33	28.2	0.34	0.0559	2.7	0.56	4.0	0.0722	3.0	449.2	13.0	446	60
A8.1	574	279	0.50	35.2	0.27	0.0589	1.9	0.58	3.5	0.0712	3.0	443.1	12.8	562	41
A9.1	472	238	0.52	31.0	0.47	0.0574	2.9	0.60	4.2	0.0762	3.0	473.3	13.7	507	64
A10.1	1460	644	0.46	94.5	0.11	0.0571	1.3	0.59	3.2	0.0753	3.0	467.8	13.4	495	28
B1.1	230	81	0.36	18.2	0.27	0.0679	2.4	0.86	3.0	0.0920	1.8	567.3	9.5	864	51
B2.1	515	210	0.42	126.6	0.15	0.1621	0.4	6.39	1.7	0.2859	1.7	1621.3	24.1	2478	6
B3.1	733	174	0.24	137.7	1.60	0.1582	2.7	4.69	8.0	0.2152	7.5	1256.4	85.4	2437	46
B4.1	363	156	0.44	124.4	0.08	0.1640	0.3	9.01	3.1	0.3986	3.1	2162.7	56.5	2497	6
B5.1	774	386	0.51	47.8	0.23	0.0538	2.5	0.53	3.1	0.0716	1.8	446.0	7.7	362	56
C1.1	449	185	0.43	129.7	0.24	0.1622	4.4	7.50	12.4	0.3355	11.5	1865.1	186.8	2478	75
C2.1	1129	501	0.46	78.5	0.06	0.0565	0.7	0.63	9.9	0.0809	9.8	501.4	47.5	473	15
C3.1	3448	3377	1.01	538.8	8.16	0.1687	8.9	3.89	13.1	0.1671	9.6	995.9	88.5	2545	150
C4.1	535	280	0.54	151.3	0.11	0.1644	1.6	7.46	6.9	0.3289	6.7	1833.2	106.7	2502	27

Footnotes can be found in Table 2.

Table 2 SHRIMP U-Pb data for the Bangxi arae metabasite sample 05BX04-2 in the northwest Hainan Island, South China

Analyzed spot	ppm U	ppm Th	$^{232}Th/^{238}U$	ppm $^{206}Pb^*$	*f*206/%	$^{207}Pb/^{206}Pb^*$	±%	$^{207}Pb^*/^{235}U$	±%	$^{206}Pb^*/^{238}U$	±%	t ($^{206}Pb/^{238}U$) (Ma)	±%
1.1	738	157	0.22	27.2	0.07	0.0546	1.8	0.32	3.5	0.0429	3.0	271.0	8.0
1.2	1325	171	0.13	48.6	1.82	0.0589	4.2	0.34	5.2	0.0419	2.9	264.8	7.6
2.1	3635	773	0.22	129.7	0.23	0.0526	1.1	0.30	3.1	0.0414	2.9	261.6	7.5
3.1	1723	291	0.17	66.8	0.10	0.0512	1.3	0.32	3.2	0.0451	2.9	284.4	8.2
4.1	728	415	0.59	26.7	0.20	0.0510	2.3	0.30	3.8	0.0426	3.0	268.7	7.8
5.1†	828	691	0.86	107.7	0.07	0.0669	1.9	1.40	3.5	0.1513	2.9	908.3	24.9
6.1	410	137	0.34	14.8	0.20	0.0526	2.8	0.30	4.2	0.0420	3.1	265.0	8.1
7.1	1405	231	0.17	54.0	0.21	0.0551	2.2	0.34	3.7	0.0446	3.0	281.4	8.1
8.1	913	180	0.20	32.7	0.59	0.0500	4.7	0.29	5.5	0.0415	3.0	262.1	7.6
9.1	883	429	0.50	32.5	0.37	0.0518	2.7	0.30	4.0	0.0427	3.0	269.7	7.8
10.1	2067	186	0.09	77.8	0.10	0.0537	2.3	0.32	6.8	0.0437	6.4	275.9	17.2
11.1	2214	325	0.15	78.9	0.59	0.0534	2.1	0.30	3.6	0.0413	2.9	260.6	7.5
12.1	1472	214	0.15	55.4	0.19	0.0505	1.8	0.30	3.4	0.0437	2.9	275.8	8.0
13.1	2132	516	0.25	78.5	0.14	0.0513	1.3	0.30	3.2	0.0428	2.9	270.1	7.8
14.1	2525	1140	0.47	54.3	0.23	0.0516	1.8	0.18	3.4	0.0250	2.9	159.1	4.6
15.1	449	297	0.68	16.2	0.82	0.0501	4.4	0.29	5.5	0.0418	3.3	264.0	8.5
16.1	1123	212	0.20	41.1	0.44	0.0579	3.8	0.34	4.8	0.0424	3.0	267.9	7.8

*Denotes radiogenic, *f*206% is the percentage of common ^{206}Pb in the total measured Pb. The common Pb and radiogenic Pb corrections are based on the measured ^{204}Pb. The measurements of U, Th, and Pb were conducted using the SHRIMP II ion microprobe at the Beijing SHRIMP Center, China.

Uncertainties given at the one σ level.

$^{207}Pb/^{206}Pb$ age for analyzed spot 5.1 †: 835 ± 39 Ma.

(*see the discussion, below*). SHRIMP-II was used for 23 spot analyses on a further 22 zircon grains from these selected samples.

Two analyzed spots A5.1 and A11.1 showed a discordance degree greater than 50% and were rejected. The other nine analyzed spots from eight zircon grains in sample TC001 give two age associations (Table 1 and Fig. 10a). (i) Two analyzed spots A1.1 and A4.1 have been carried out on zircon domains of one zircon grain and yield approximate SHRIMP zircon $^{207}Pb/^{206}Pb$ ages of 1442 ± 23 Ma and 1453 ± 10 Ma (1ó), respectively. (ii) The other seven analyzed spots from seven zircon grains produce concordant to approximately concordant $^{206}Pb/^{238}U$ ages spanning from 442.1 ± 13.7 Ma to 514.3 ± 30.2 Ma with a weighted U-Pb mean age of 445 ± 14 Ma (MSWD = 0.057).

Two analyzed spots B6.1 and C5.1 showed a discordance degree greater than 50% and a percentage of common ^{206}Pb more than 5%, and thus they were rejected. The other nine analyzed spots carried out on nine zircon grains in samples YSY03 and YSY05-2 yield three age associations (Table 1 and Fig. 10b). (i) Six analyzed spots from six zircon grains give a weighted $^{207}Pb/^{206}Pb$ mean age of 2488.1 ± 8.3 Ma (MSWD = 1.35). (ii) Two spots on two zircon grains give concordant U-Pb ages of 446.0 ± 7.7 Ma (1ó) and 501 ± 47.5 Ma (1ó), respectively. (iii) One spot B1.1 on one zircon grain with broad zoning yields an approximately concordant U-Pb age of 567.3 ± 9.5 Ma (1ó) with a $^{207}Pb/^{206}Pb$ age of 864 ± 51 Ma (1σ).

THE BANGXI AREA METABASITES

Fifty-four zircon crystals, which have a size ranging from 50 to 200 μm in length and from 50 to 100 μm in width, were recovered from the Bangxi area metabasite sample 05BX04-2. Most of zircons in this sample are colorless, transparent, euhedral and prismatic, and contain a very clear, homogeneous, and well-preserved oscillatory zoning (Fig. 9). One grain (the analyzed spot 5.1 in Fig. 9) consists of an inherited core surrounded by an oscillatory domain of magmatic origin. For a few grains, faint or ghost oscillatory zoning is also observed, and is interpreted as various degree of lead loss. Thus the CL-patterns and morphology of zircon in the Bangxi area metabasites are distinct from those of zircons observed in the Tunchang area metabasites.

SHRIMP-II was used for 17 spot analyses on a further 17 zircon grains from the sample 05BX04-2. The results show that the analyzed spots yielded three age associations (Table 2 and Fig. 11). (i) 15 analyzed spots on 15 zircon grains with oscillatory zoning give a concordant to approximately concordant $^{206}Pb/^{238}U$ age range of from 260.6 ± 7.5 Ma to 284.4 ± 8.2 Ma with a weighted concordant U-Pb mean age of 269 ± 4 Ma (MSWD = 0.78). (ii) One spot on one zircon

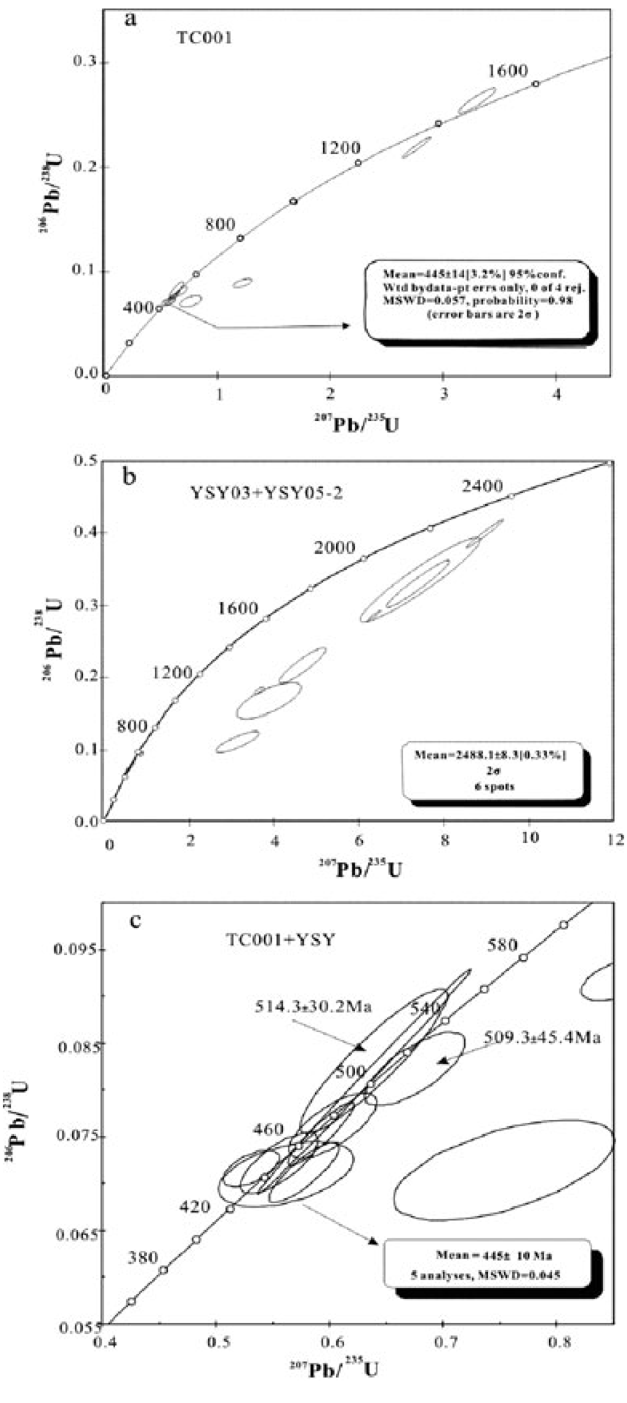

Fig. 10 U-Pb Concordia diagrams of zircons in the Tunchang area metabasite samples TC001, YSY03 and YSY05-2 from the east-central island (a: for the sample TC001, b: for the samples YSY03 and YSY05-2, and c: for samples TC001, YSY03 and YSY05-2).

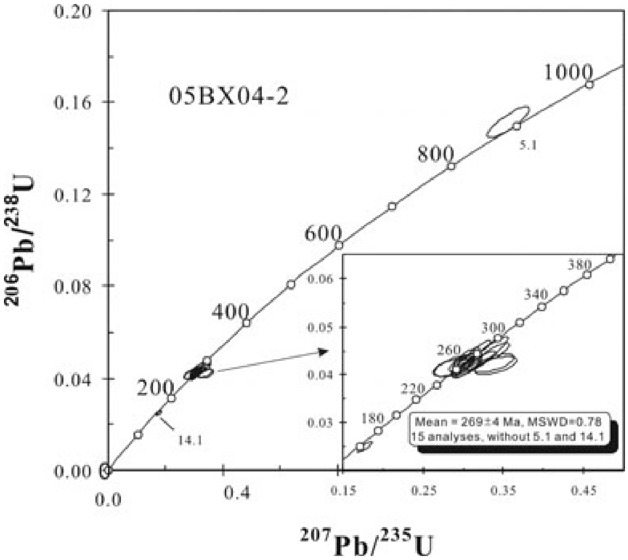

Fig. 11 U-Pb Concordia diagram of zircons in the Bangxi area metabasite sample 05BX04-2 from the northwest island.

core with broad zoning yields an approximately concordant $^{207}Pb/^{206}Pb$ age of 835 ± 39 Ma (1σ). (iii) One spot on one zircon core with oscillatory zoning gives a rather young concordant U-Pb age of 159.1 ± 4.6 Ma.

DISCUSSIONS

Li *et al.* (2002) suggested that both the Chenxing (i.e. Tunchang) area and the Bangxi area metabasites had a derivation of their primitive magma from an NMORB-type mantle source. A Sm-Nd isochronic age of *ca* 333 Ma also was yielded by the whole rock samples from both the areas and interpreted as the protolith age for these rocks. They thus postulated that these metabasites were relics of the Paleo-Tethys and that the east–west-tending Changjiang-Qionghai fault zone (Fig. 1b) was a sutured location due to the collision of southern Hainan Island (part of Indochina) with northern Hainan Island (part of south China). Our studied results, however, have revealed that the Tunchang area metabasites are distinct from the Bangxi area metabasites not only in the geochemical and isotopic compositions, but also in the protolith natures and ages, implying these rocks most likely recorded a different tectono-magmatic-metamorphic event.

TIMING OF PROTOLITH

In metabasites, Schulz *et al.* (2006) suggested that zircon Th/U is 0.9–1.6 for the within plate basalt (WPB)-type sample, 0.2–0.9 for the volcanic arc basalt (VAB)-type rocks and 0.03 for the NMORB-type eclogitic amphibolite, reflecting its dependence on and increasing with whole rock Th/U. Especially, ophiolitic meta-mafic/ultramafic rocks are highly variable in Th/U ratios for zircons. For examples, a Th/U ratio ranges from <0.01–15.60 for zircons in the Zermatt-Saas-Fee (Alps) ophiolitic metagabbros (Rubatto *et al.* 1998), from 0.33 to 1.61 for zircons in the Switzerland metamafic/ultramafic rock association (Schaltegger *et al.* 2002), and from 0.47 to 1.02 for zircons in the southern Brasi'lia belt (central Brazil) amphibolites (Piuzana *et al.* 2003). Liati *et al.* (2002, 2003, 2004) also reported a broad Th/U range of from 0.005 to 1.03 for zircons in the UHP garnet-rich mafic rocks of the Rhodope zone (Greece), from 0.01 to 1.12 for zircons in the ophiolitic amphibolites of the Alps, and from 0.002 to 0.78 for zircons in the ophiolitic rocks of the Hellenides (mainland Greece). Hence, the Th/U ratio needs to be treated with caution as a criterion to distinguish igneous and metamorphic/recrystallized zircon in metamorphic igneous rocks, especially in metabasites.

THE BANGXI AREA METABASITES

As the summary above, the Bangxi area metabasites in the northwest island have variable but relatively high Zr contents, and so that yielded abundant zircon crystals; consistent with petrographical and mineralogical observations. The Th/U ratios (0.13–0.83), the U concentrations (generally $\geq 410 \times 10^{-6}$: Table 2) and the internal structures of zircons commonly characterize most of the zircons in these metabasites as typical magmatic petrogenetic zircons (e.g. Vavra *et al.* 1996; Belousova *et al.* 2002). The suggested protoliths and the geochemical affinities of these metabasites to OIBs and/or MORBs (Fig. 5c) also imply that the magma generation was related to breakup of continental lithosphere followed by formation of an ocean crust due to mantle plume activity (e.g. Francis 1995; Revillon *et al.* 1999). Thus the weighted concordant $^{238}U/^{206}Pb$ mean age of 269 ± 4 Ma yielded by 15 analyzed spots on zircon domains in sample 05BX-04–2 should represent the most precious forming time, reflecting their emplacement at the early Permian. However, the zircon with $^{207}Pb/^{206}Pb$ age of 835 ± 39 Ma probably is inherited from the host rocks, whereas the zircon with concordant U-Pb age of 159.1 ± 4.6 Ma most likely is from contamination due to mineral separation.

THE TUNCHANG AREA METABASITES

Based on the CL images and SHRIMP II analysis, most of the zircons in the Tunchang area metabasites are characterized by oscillatory and/or broad zoning, and have Th/U ratios of ranging from 0.23 to 0.98 (Table 1), implying a derivation of these zircons from magma crystallization. However, the low Zr concentration in most of the Tunchang area metabasites, especially in samples YSY05-2 (10.1×10^{-6}) and YSY03 (9.9×10^{-6}) by ICP-MS analysis (Xu *et al.* 2007; in review), being comparable to that in primitive mantle (11.2×10^{-6}: Sun & McDonough 1989), reflects that these zircons probably are comagmatic due to igneous crystallization (Liati *et al.* 2002, 2003).

The zircon in the Tunchang area metabasites further can be grouped into three types, based on CL patterns, morphology and isotopic analysis of 23 zircon domains/zircon grains. Type 1 is characterized not only by an internal structure of homogeneous, clear, well-preserved oscillatory zoning (Fig. 7), but also by a high Th/U ratio of ranging from 0.32 to 0.72, as is the case for melt precipitated crystals (Liati *et al.* 2002, 2003). A few zircons show gray-white and/or white mantle or core in CL images, and contain faint or ghost oscillatory zoning, being due probably to (partial) recrystallization ascribed to high temperatures (T) in the presence of high amounts of fluids (Liati *et al.* 2004). Thus the weighted U-Pb mean age of 445 ± 10 Ma (MSWD = 0.045: Fig. 10c) yielded by the five analyzed spots on Type 1 zircon domains probably reflect a minimum time of magmatic crystallization, because the $^{206}Pb/^{238}U$ age range of from *ca* 440 to *ca* 514 Ma encompasses both the time of igneous crystallization and immediately following high-T metamorphism in a high-T shear zone after their formation. Type 2 has a broad or oscillatory but faint or ghost zoning represented by the alternating presence of gray- (high U) with bright- (low U) sectors. Radiating and zoning fractures also are well developed in this type, which partly contains resorbed shapes or other mineral inclusions (Fig. 8). Thus Type 2 is inherited magmatic zircon but was affected by high-T fluid metamorphism. This is an additional indication that the protoliths of the Tunchang area metabasites more likely were a subvolcanic rock or a dyke (e.g. diabase or fine-grained gabbro) and/or a basalt, where zircons could not grow large in the relatively rapidly cooling basic melt (Liati *et al.* 2003). For Type 3 with the $^{207}Pb/^{206}Pb$ age value of *ca* 1450 Ma (A1.1 and A4.1 in Fig. 7), majority of them consist largely of an oscillatory zoned, magmatically formed domains surrounded by a very thin metamorphic rim, bright in CL images. The crystal size (about 150 μm long and 100 μm) as well as the relatively euhedral shape of the zircon, also favor the interpretation of the zircon as comagmatic zircon.

ORIGIN OF THE INHERITED ZIRCONS

Precambrian, especially the Neoarchean-Paleoproterozoic inherited zircons occur widely in the Tunchang area metabasites, the east-central island. These inherited zircons also are characterized by typically magmatic zoning of zircon and high Th/U ratio (0.23*ca* 0.98: Table 1), which resemble the inherited zircon generally present in ophiolitic mafic magma (e.g. Pilot *et al.* 1998; Rubatto *et al.* 1998; Liati *et al.* 2002, 2003, 2004). These workers interpreted these inherited magmatic zircons as a result of: (i) underplated subcontinental lithospheric mantle due to rifting leading to oceanization, or (ii) assimilated mafic magma by subducted continental crust, or (iii) previously crystallized zircon in the mantle and then were carried up by mafic melts, and/or (iv) zircons in ocean floor sediments trapped in basaltic magma when ophiolitic magma went up to ocean floor. Liati *et al.* (2003) further suggested that the presence of abundant inherited zircons in ophiolitic rocks indicates partial mantle melting within subcontinental mantle or generally MORB-type mantle close to a continental margin, favoring the proximity of an ophiolitic unit to thinned continental crust. The geochemical and isotopic characteristics imply an intraoceanic arc or a supra-subduction zone-like setting for the protoliths of the Tunchang area metabasites. Thus these inherited zircons with signature of magmatic zircon most likely are interpreted as a derivation from partial melting of MORB-type mantle close to a continental margin.

IMPLICATIONS FOR THE GEODYNAMIC EVOLUTION OF SOUTH CHINA

CONNECTIONS OF SOUTH CHINA WITH EAST GONDWANA

Recent geochronological studies both in the Pan-African and Braziliano belts (e.g. Schmitt *et al.* 2004 and references therein) indicate the assembly of Gondwana was only completed by the end of the Cambrian and Early Ordovician. The peak for assembly of the Gondwana was between 505 and 518 Ma whereas between 490 and 450 Ma for orogenic collapse (Fitzsimons 2000; Boger & Miller 2004). The assembly of the east Gondwana, which had been accompanied by various subduction-accretion and collision events, was multiphase and had a time interval of between *ca* 750 and *ca* 500 Ma (Meert 2003). Wilde *et al.* (2003) and Jacobs *et al.* (2003) also noted that the terrenes sourced from east Gondwana appear commonly to show a metamorphic peak at *ca* 500 Ma. Obviously, these age values are less compatible with the minimum age of crystallization for protoliths of the Tunchang area metabasites in the east-central Hainan Island, South China, appearing to imply that Hainan Island is unlikely to have been attached to Australian Gondwana during the entire Cambrian-Ordovician. However, trilobite faunal affinities suggest that the South China block (including Hainan Island), the North China block and the Siberia Craton had drifted close to the Australia-East Antarctica margin of Gondwana during the Early and Middle Cambrian (Li 1998 and references therein). Geological observation also reveals that the early Paleozoic volcanic-clastic sedimentary rocks in Sanya area, the southeast island (Fig. 1b) are comparable to those in the late Proterozoic-early Cambrian Tasmania fold belt terrene (Zeng *et al.* 1992). Thus, Hainan Island when the Gondwana was formed by the Early Cambrian most likely was part of the northern extension of the continental ribbon including Tasmania and South China block adjacent to the eastern Australia mainland (Fig. 12). If so, the westward subduction of the Paleo-Pacific ocean during the Cambrian along the eastern margin of Australia-Antarctica (Li & Powell 2001), probably had an important influence on the Paleozoic tectonic development of Hainan Island. The metavolcanic rocks with continental arc signatures, which occurred as interlayer with the early Paleozoic felsic schists in Tunchang area, the east-central island, have a zircon U-Pb age of 528 ± 48 Ma (Ding *et al.* 2002), heralding such the subduction event at that time.

THE NATURE FOR THE CALEDONIAN OROGENY IN SOUTH CHINA

The nature of the intensive Caledonian Orogeny during the early Paleozoic in the region between the Yangtze and the Cathaysian blocks of South China (Li 1998), is still unclear. More and more evidence indicate the possible consumption of substantial oceanic crust during this orogeny, probably suggesting the Caledonian Orogeny was not intracontinental in nature, but characterized by various subduction-accretion and collision events. The widespread outcrops of the late Precambrian-early Paleozoic (*ca* 590–460 Ma) ophiolitic mélanges and associated volcanic arc rocks along both sides of the Zhenghe-Dapu deep fault zone in South China (Yang *et al.* 1995; Ren *et al.* 1997a,b; also see: Fig. 13), indicate a Sinian-Cambrian subduction-accretion. The Sinian-early Paleozoic (*ca* 460–540 Ma: Ding *et al.* 2005 and references; Peng *et al.* 2006a) volcanic-clastic sedimentary rocks of deep-water facies with arc geochemical affinities and the synchronous arc-type granites in the region between the Yangtze and the Cathaysian blocks, in fact, accounted for the synchronous occurrence of a back-arc basin (Qiu *et al.* 1996). The abundant, syn-collisional S-type granites (HBGMR 1988; Wang *et al.* 1999; Ding *et al.* 2005; Peng *et al.* 2006a), and the widespread granulite facies metamorphism recorded by these granitic rocks in the region between the Cathaysian and the Yangtze blocks (Chen & Zhuang 1994), also reveal the collisional

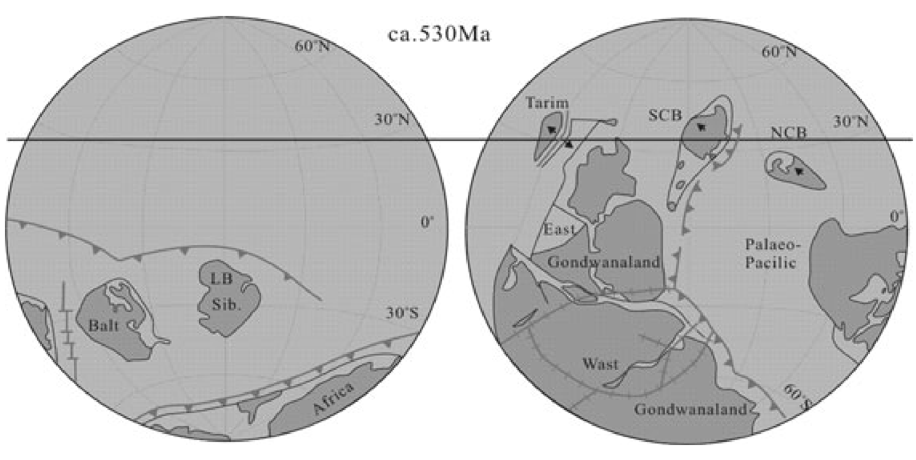

Fig. 12 Simplified map of East Gondwana at *ca* 530 Ma showing the inferred position of South China (including Hainan Island), modified after Li & Powell 2001). SCB: South China block; NCB: North China block.

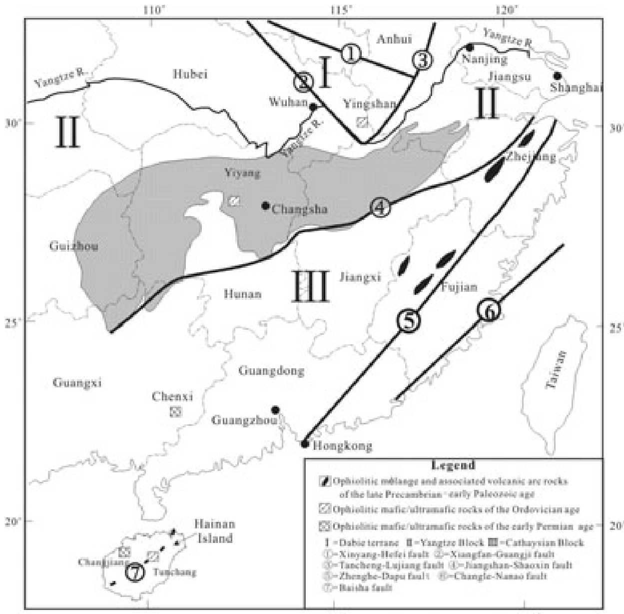

Fig. 13 Simplified map of South China showing the tectonic relationship between the Yangtze and the Cathaysian blocks, and the possible occurrences of ophiolitic rocks with Paleozoic age, modified after Chen and Jahn (1998). The shaded area represents the exposed Mesoproterozoic-Neoproterozoic volcanic-clastic sedimentary rocks in the southeast margin of the Yangtze block.

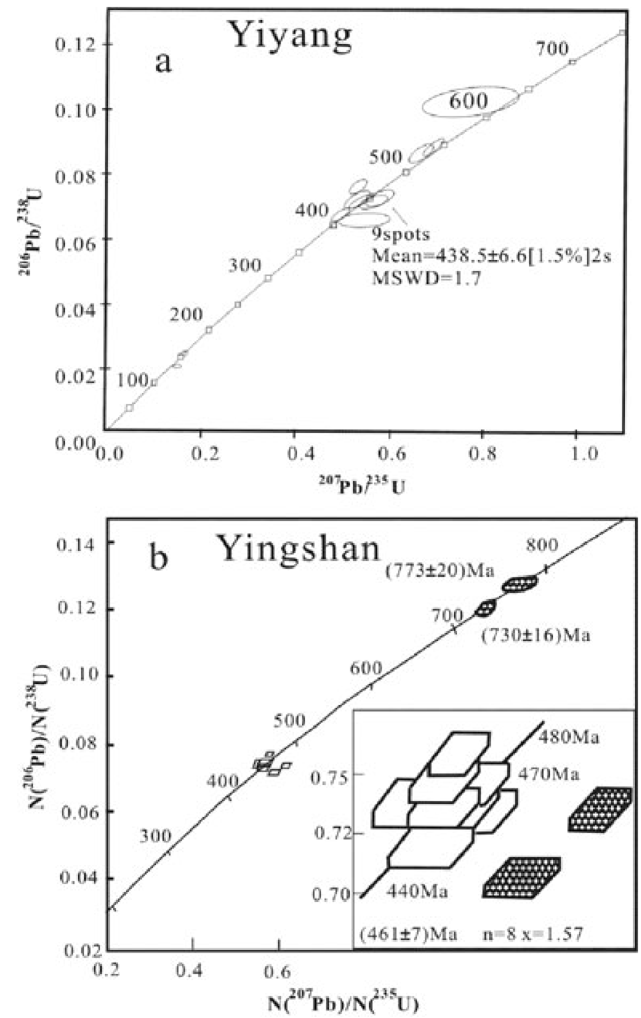

Fig. 14 Concordia diagrams of signal zircon SHRIMP U-Pb dating for both the ophiolitic mafic/ultramafic rocks from Yiyang area, Hunan Province (a: after Jia & Peng 2005) and the eclogitic ophiolitic rocks from Yingshan area, Hubei Province (b: after Gao *et al.* 2002), respectively.

orogeny at a dominant time of *ca* 435–400 Ma. This is in agreement with the observation that the Pre-Carboniferous rocks in South China (including Hainan Island) were strongly deformed, and that the underlying early Paleozoic rocks generally have a high-angular unconformity with the overlying Carboniferous rocks (Wang *et al.* 1991). Moreover, the gabbroic rocks in the Yunkai area between the Guangdong and Guangxi Provinces, South China probably marked the orogenic detachment at *ca* 400 Ma (Peng *et al.* 2006b).

The most significant is the possible presence of an Ordovician oceanic crust in the region between the Yangtze and the Cathaysian blocks of South China. On the basis of SHRIMP U-Pb dating on zircon in the ophiolitic metamafic/ultrmafic rocks of the Yiyang area, Hunan Province of the Yangtze block (Fig. 13), nine analyzed zircon domains yielded a concordant $^{206}Pb/^{238}U$ age range of from 434 ± 11 Ma to 539 ± 13 Ma with a weighted U-Pb mean age of 438.5 ± 6.6 Ma (MSWD = 1.7: Fig. 14a). The eight analyzed zircons in the eclogitic ophiolitic rocks of the Yingshan area, Hubei province of the Dabie terrane (Fig. 13) which has been considered as a northern part of the Yangtze block (Chen & Jahn 1998) also gave a concordant $^{206}Pb/^{238}U$ age range of from 440 ± 5 Ma to 471 ± 5 Ma with a weighted U-Pb mean age of 461 ± 7 Ma (MSWD = 1.57: Fig. 14b). The Yiyang metamafic/ultrmafic rocks appear to occur in the Mesoproterozoic volcanic-clastic sedimentary rocks (Fig. 15a), thus they are often interpreted as a Mesoproterozoic age (*ca* 1300 Ma by whole rock Sm-Nd method: Liu 1994; Tang *et al.* 1997) or as an older, Archean-Paleoproterozoic age (*ca* 3000–1800 Ma by whole rock Sm-Nd method: Guo *et al.* 2003). However, field observation shows that these rocks not only are present as lensoid or stratiform-like bodies within the Mesoproterozoic host rocks, but also show a fault contact with the latter (Fig. 15b), clearly indicating their inclusion in a mélange (e.g. Rao *et al.* 1993; Jia & Peng 2005). In connection with their complex metamorphism, the suggested protolith age for the metamafic/

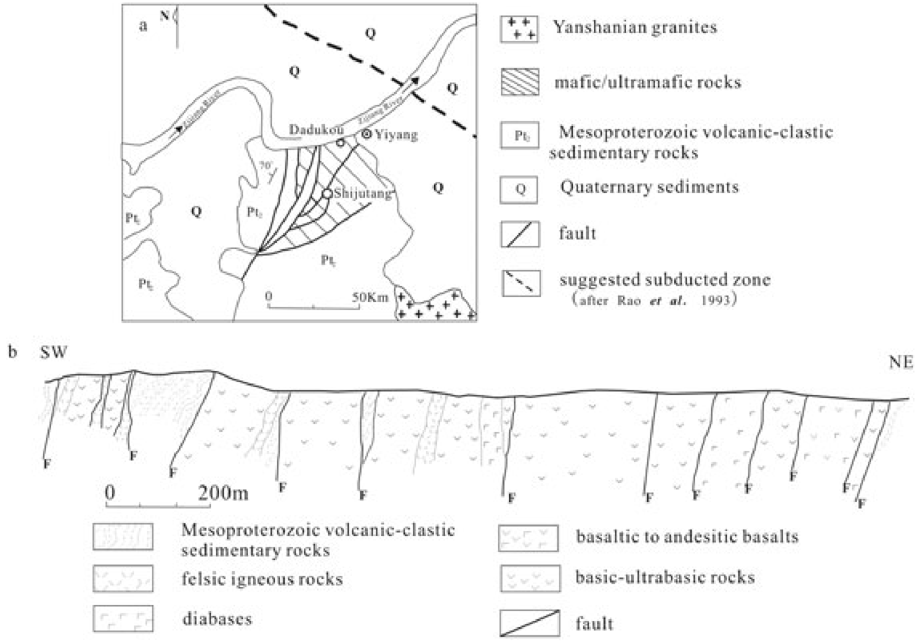

Fig. 15 Sketch map showing regional geology of the ophiolitic mafic/ultramafic rocks in Yiyang area, Hunan Province (a), and their relationship to host rocks (b).

ultramafic rocks in the Yiyang area needs to be reconsidered. Indeed, the analyzed zircon domains and/or zircon grains by Jia and Peng (2005) are extremely similar in CL patterns and morphologies to these in the Tunchang area metabasites, the east-central Hainan Island, because the zircon domains/zircon crystals with the concordant U-Pb age of *ca* 450 Ma are characterized not only by a very clear, homogeneous, oscillatory zoning in CL images, but also by high Th/U ratios (generally between 0.2 and 0.66). Abundant inherited zircons with $^{207}Pb/^{206}Pb$ apparent ages of ranging from *ca* 920–3000 Ma also are recovered from these rocks. Thus the age of *ca* 450 Ma can be interpreted as the minimum age of crystallization for the protoliths of the metamafic/ultramafic rocks in the Yiyang area. The eclogitic ophiolitic rocks in Yingshan area (e.g. Zhang *et al.* 1995; Gao *et al.* 2002) are similar in field geology, geochemistry and isotope to those of the metamafic/ultramafic rocks in the Yiyang area. Similarly, the zircon crystals with a Th/U ratio of ranging from 0.32 to 1.55 (cf. Gao *et al.* 2002) probably are comagmatic and the minimum age for protoliths of these rocks should be *ca* 460 Ma. Thus the age of *ca* 450 Ma for the time of crystallization of the protoliths of the metabasites with oceanic (MORB) geochemical affinities from the Yangtze block and the Hainan Island, record the oceanic magmatism, although they were interpreted earlier and/or younger as remnants of ophiolitic orogin.

THE CONNECTION OF THE PALEO-TETHYS WITH SOUTH CHINA

The boundaries between the Gondwana-derived East and Southeast Asian continental terranes are marked by suture zones recognized by the presence of ophiolites, mélanges and accretionary complexs, representing the opening and closing of successive Tethys oceans, i.e. the Paleo-, Meso- and Ceno-Tethys oceans (Metcalfe 1996, 2000). The Jinshajiang ophiolitic rocks and their Ailaoshan equivalents in the Honghe-Ailaoshan sutured zone (Fig. 1a) due to the collision between the Indochina and the South China blocks have time intervals of *ca* 330–280 Ma and *ca* 360–260 Ma, respectively, based on SHRIMP U-Pb dating on zircon in the ophiolitic rocks and associated granitic rocks (Jian *et al.* 2003a,b). Zhang *et al.* (1994) also proposed a small oceanic basin, likely responding to slow-spreading ridge, was responsible for the generation of the Shuanggou ophiolites in the Honghe-Ailaoshan zone. The late Paleozoic island arc-type basaltic rocks in the Chenxi area, Guangxi Provinces, South China (Fig. 13) which represented the products due to the subduction of Paleo-Tethys under the South China continental margin, had an extrusive age of *ca* 261 Ma (Zhang *et al.* 1997b). In Hainan Island, the typically calc-alkaline I-type granites formed in an active continental margin in the Qingzhong area have a SHRIMP zircon U-Pb age of 267–262 Ma (Li *et al.* 2006). We thus sug-

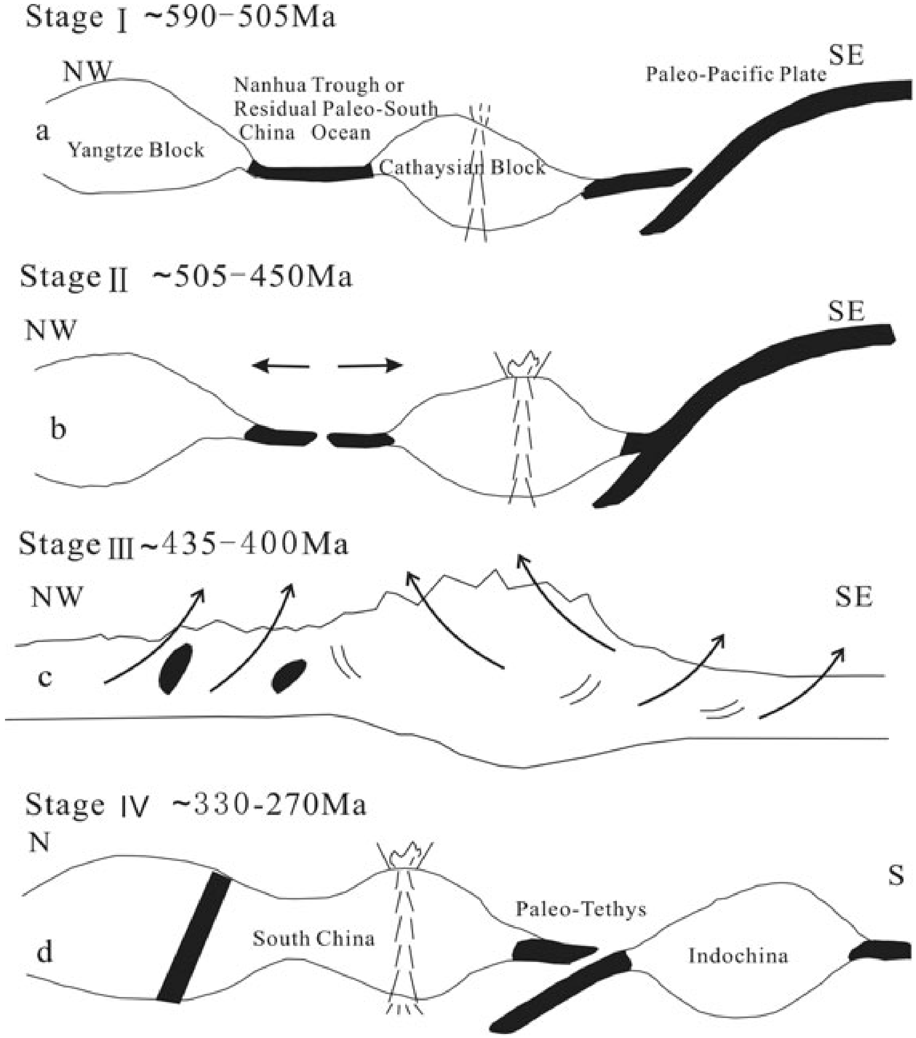

Fig. 16 Schematic diagrams show the possible tectonic development of South China since the late Precambrian: (a) subduction stage of the Paleo-Pacific plate; (b) expanding stage of the back-arc basin; (c) collisional stage of the Yangtze block with the Cathaysian block and (d) subduction stage of the Paleo-Tethys. Nanhua trough and Paleo-South China ocean in the figure are cited from Li *et al.* (1999) and Guo *et al.* (1985), respectively.

gested the subduction of the Paleo-Tethys beneath the South China continental margin probably led to the opening of back-arc basin, the subsequent formation of a small oceanic basin and the generation of *ca* 270 Ma protoliths for the Bangxi area metabasites along the Changjiang-Qionghai fault zone in Hainan Island. The widespread Hercynian-Indosinian syncollisional S-type granites in Hainan Island more likely propagated the closure of the eastern part of Paleo-Tethys in South China during the late Permain-earliest Triassic.

A POSSIBLE MODEL FOR THE GEODYNAMIC EVOLUTION OF SOUTH CHINA SINCE THE LATE PRECAMBRIAN

It is a rather common feature in ophiolites worldwide that intraoceanic thrusting may take place while the slow-spreading mid-oceanic ridge is still active (or immediately afterwards), which leads to heat responsible for the metamorphic overprint (for a review see: Liati *et al.* 2004). This implies that magmatic crystallization is quasi-synchronous to the high-T overprint. The internal structures of zircons from and the intensive shear-related deformation in the Tunchang area metabasites support that idea that the zircons originally crystallized in the gabbro-related protoliths and were (partially) recrystallized immediately afterwards in the high-T shear zone. We thus suggest that the subduction of an intraoceanic arc at the middle to late Ordovician which was accompanied by the quasi-synchronous spreading of mid-oceanic ridge, probably had taken place in the region between the Yangtze and the Cathaysian blocks of South China.

Based on the various age data and above discussion, herein, a geodynamic model is proposed to describe the geodynamic evolution of South China since the late Precambrian (Fig. 16). The main geotectonic domains involved in this model are the Paleo-Pacific plate, the Cathaysian block (including Hainan Island), the Nanhua trough or the residual Paleo-South China ocean, the Yangtze block, the

Paleo-Tethys and the Indochina block. The westward subduction of the Paleo-Pacific plate beneath the South China continental margin during the late Precambrian-Cambrian led to the occurrence of a continental margin arc system (Fig. 16a). The backarc basin probably covered the position of the Nanhua trough (Li *et al*. 1999), or the residual Paleo-South China ocean (Guo *et al*. 1985). The subsequent extension of the basin was due probably to the quick impingement of a mantle plume on the oceanic mantle triggered by the subducted slab. The extreme extension led to the generation of a middle to late Ordovician intraoceanic arc in the basin (Fig. 16b). The ocean basin probably was mature and large, because the subduction of the intraoceanic arc at *ca* 435–400 Ma was accompanied quasi-synchronously by activity of a slow-spreading mid-oceanic ridge, and the basin closure led to the overthrusted ophiolitic rocks into the South China and the widespread, syncollisional S-type granites in the region between the Yangtze and the Cathaysian blocks (Fig. 16c). Afterwards, the drift of the Gondwana-derived Indochina northwards to the South China and the subduction of the Paleo-Tethys beneath the southern continental margin of South China during the early Carboniferous-early Permian probably induced a continental margin arc system (Fig. 16d). The further extension of the younger backarc basin at last resulted in the formation of a small oceanic basin, which were represented by the *ca* 270 Ma mafic/ultrmafic rocks in the southern continental margin of South China.

CONCLUSIONS

SHRIMP U-Pb dating of zircon domains/crystals assisted by CL images, in combination with geological, petrographical and geochemical data revealed the following features of the metabasites within the Paleozoic volcanic-clastic sedimentary sequences in Hainan Island, South China:

1 The protoliths for the Tunchang area metabasites in the east-central Hainan Island probably are composed of gabbroic rocks, gabbroic to diabasic rocks and pillow lava, which most likely represent the upper layers of an incomplete, dismembered ophiolite body. The Bangxi area metabasites in the northwest Hainan Island have a protolith nature probably containing pillowed lava, gabbroic rocks and/or picritic rocks.

2 The minimum age of *ca* 450 Ma for the magmatic protoliths of the Tunchang area metabasites recorded the formation of an intraoceanic arc. The presence of abundant inherited zircons in these rocks clearly indicates their protoliths were originally derived from a MORB-type mantle close to a continental margin. In contrast, the *ca* 270 Ma age for the magmatic protoliths of the Bangxi area metabasites most likely marked the formation of a small, oceanic basin due to the subduction of the Paleo-Tethys beneath the southern continental margin of South China.

3 The early Paleozoic ocean between the Yangtze and the Cathaysian blocks, South China, was due to further spreading of the late Neoproterozoic Nanhua trough or the residual Paleo-South China ocean initiated by the subduction of the Paleo-Pacific ocean and subsequent or synchronous impingement of a mantle plume. Thus, the Caledonian Orogeny in South China probably was not intracontinental in nature, but characterized by various subduction-accretion and collision events.

ACKNOWLEDGEMENTS

We would like to thank Professor Chen Zuofen and Professor Ding Shijiang for their help in field investigation. Constructive comments from Professor Ming-Guo Zhai, Professor Mei-Fu Zhou, Professor Xian-Hua Li, Professor Simon Wallis and another anonymous reviewer are gratefully acknowledged. We are also grateful to Professor Wan Yusheng for his instruction on SHRIMP zircon U-Pb dating. A particular thank is given to Professor Mao Qian for his help in CL imaging. This study was financially cosupported by Chinese Academy of Sciences (KZCX2-YW-203-2 and GIGCX-04-04) and Chinese Natural Science Fundation Committee (No. 40473017).

REFERENCES

Belousova E. A., Griffin W. L., O'Reilly S. Y. & Fisher N. I. 2002. Igneous zircon: Trace element composition as an indicator of source rock type. *Contributions to Mineralogy and Petrology* **143**, 602–22.

Black L. P., Kamo S. L., Allen C. M. *et al.* 2003. TEMORA 1: A new zircon standard for Phanerozoic U-Pb geochronology. *Chemical Geology* **200**, 155–70.

Boger S. D. & Miller J. M. 2004. Terminal suturing of Gondwana and the onset of the Ross-Delamerian Orogeny: The cause and effect of an Early Cambrian reconfiguration of plate motions. *Earth and Planetary Science Letters* **219**, 35–48.

CHEN B. & ZHUANG Y. X. 1994. The petrology and petrogenesis of Yunlu charnockite and its granulite inclusion, western Guangdong, south China. *Acta Petrologica Sinica* **10** (**2**), 139–50 (in Chinese with English abstract).

CHEN H. H., SUN S., LI J. L. *et al.* 1994. Paleomagnetic constrains on early Trissic tectonics of South China. *Scientia Geologica Sinica* **29** (**1**), 1–9 (in Chinese with English abstract).

CHEN J. F. & JAHN B. M. 1998. Crustal evolution of southeastern China: Nd and Sr isotopic evidence. *Tectonophysics* **284**, 101–33.

CHEN J. F., FOLAND K. A., XING F. M., XU J. & ZHOU T. X. 1991. Magmatism along the southeast margin of the Yangtze block: Precambrian collision of the Yangtze and Cathaysia blocks of China. *Geology* **19**, 815–18.

DING SJ., XU CH., LONG W. G., ZHOU Z. Y. & LIAO Z. T. 2002. Tectonic attribute and geochronology pf metavolcanic rocks, Tunchang, Hainan Island. *Acta Petrologica Sinica* **18**, 83–90 (in Chinese with English abstract).

DING X., ZHOU X. M. & SUN T. 2005. The episodic growth of the continental crustal basement in South China: Single zircon LA-ICPMS U-Pb dating of Guzhai Granodiorite in Guangdong. *Geological Review* **51** (**6**), 382–92 (in Chinese with English abstract).

FANG Z., ZHAO J. X. & MCCULLOCH M. T. 1992. Geochemical and Nd isotopic study of Paleozoic bimodal volcanicsin Hainan Island, South China-implications of rifting tectonics and mantle reservoirs. *Lithos* **29**, 127–39.

FITZSIMONS I. C. W. 2000. A review of tectonic events in the East Antarctic Shield and their implications for Gondwana and earlier supercontinents. *Journal of African Earth Sciences* **30** (**1**), 3–23.

FRANCIS D. 1995. The implications of picritic lavas for the mantle sources of terrestrial volcanism. *Lithos* **34**, 89–105.

GAO S., QIU Y. M., LING W. L. *et al.* 2002. SHRIM P single zircon U-Pb geochronology of eclogites from Yingshan and Xiongdian. *Earth Sciences* **27** (**5**), 558–64 (in Chinese with English abstract).

GUO L. Q., TANG X. S. & PEN H. Q. 2003. The Sm-Nd isotopic ages of the Early Precambrian mafic-ultramafic volcanic rocks in Yiyang, Hunan. *Geology and Mineral Resources of South China* **2**, 46–51 (in Chinese with English abstract).

GUO L. Z., SHI Y. S., MA R. S., LU H. F. & YE S. F. 1985. Plate movement and crustal evolution of the Jiangnan Proterozoic mobile belt, SE China. *Earth Science of Journal of Geological Society of Japan* **2**, 156–66.

GUO L. Z., LU H., SHI Y. S. *et al.* 1996. On the Meso-Neoproterozoic Jiangnan island arc: Its kinematics and dynamics. *Geological Journal of China Universities* **2**, 1–13 (in Chinese with English abstract).

HBGMR (HUNAN BUREAU OF GEOLOGY AND MINERAL RESOURCES). 1988. *Regional Geology of Hunan Province*. Geological Publishing House, Beijing (in Chinese with English abstract).

HSÜ K. J., LI J. L., CHEN H. H., WANG Q. C., SUN S. & SENGÖR A. M. C. 1990. Tectonics of South China: Key to understanding west Pacific geology. *Tectonophysics* **183**, 9–39.

HSÜ K. J., SUN S., LI J. L., CHEN H. H., PEN H. P. & SENGÖR A. M. C. 1988. Mesozoic overthrust tectonics in south China. *Geology* **16**, 418–21.

JACOBS J., FANNING C. M. & BAUER W. 2003. Timing of Grenville-age vs. Pan-African medium- to high grade metamorphism in western Dronning Maud Land (East Antarctica) and significance for correlations in Rodinia and Gondwana. *Precambrian Research* **125**, 1–20.

JAHN B. 1986. Mid-ocean ridge or marginal basin origin of the East Taiwan ophiolite: Chemical and isotopic evidence. *Contributions to Mineralogy and Petrology* **92**, 194–206.

JIA B. H. & PENG H. Q. 2005. *The Precambrian Geology in the Northeast Hunan Province and its Mineralization*. Geology Press, Beijing (in Chinese).

JIAN P., LIOU D. Y. & SUN X. M. 2003a. SHRIMP dating of Carboniferous Jinshajiang ophiolite in Western Yunnan and Sichuan: Geochronological Constraints on the evolution of the Paleo-Tethys oceanic crust. *Acta Geologica Sinica* **77** (**2**), 217–28 (in Chinese with English abstract).

JIAN P., LIU D. Y., ZHANG Q. *et al.* 2003b. SHRIM P dating of ophiolite and Leucocratic rocks within ophiolite. *Earth Science Frontiers* **10** (**4**), 439–56 (in Chinese with English abstract).

LI S. X., YUN Y., FAN Y. & ZHOU J. B. 2005. Zircon U-Pb age and its sgnificance for Qiongzhong pluton in Qiongzhong area, Hainan Island. *Geotectonica et Metallogenia* **29** (**2**), 227–33 (241) (in Chinese with English abstract).

LI X. H., ZHOU H. W., CHUNG S. L. *et al.* 2002. Geochemical and Sm-Nd isotopic characteristics of metabasites from central Hainan Island, South China and their tectonic significance. *Island Arc* **11**, 193–205.

LI X. H., LI Z. X., LI W. X. & WANG Y. J. 2006. Initiation of the Indosinian Orogeny in South China: Evidence for a Permian Magmatic Arc on Hainan Island. *Journal of Geology* **114**, 341–53.

LI Z. X. 1998. Tectonic history of the major East Asian lithospheric blocks since the mid-Proterozoic – a synthesis. Mantle dynamics and plate interactions in East Asia. *Geodynamics* **27**, 221–43.

LI Z. X. & POWELL C. M. 2001. An outline of the palaeogeographic evolution of the Australasian region since the beginning of the Neoproterozoic. *Earth Science Reviews* **53**, 237–77.

LI Z. X., LI X. H., KINNY P. D. & WANG J. 1999. The breakup of Rodinia: Did it start with a mantle plume beneath South China? *Earth and Planetary Science Letters* **173**, 171–81.

LI Z. X., LI X. H., KINNY P. D., WANG J., ZHANG S. & ZHOU H. 2003. Geochronology of Neoproterozoic synrift magmatism in the Yangtze Craton, South China and correlations with other continents: Evidence for a mantle superplume that broke up Rodinia. *Precambrian Research* **122**, 85–109.

LIANG X. Q., FAN W. M. & XU D. R. 2000. Sm-Nd age of Tunchang basaltic komatiites and its geological significance in Hainan Island. *Scientia Geologica Sinica* **35**, 240–4 (in Chinese with English abstract).

LIATI A., GEBAUER D. & WYSOCZANSKI R. 2002. U-Pb SHRIMP-dating of zircon domains from UHP garnet-rich mafic rocks and late pegmatoids in the Rhodope zone (N Greece); evidence for Early Cretaceous crystallization and Late Cretaceous metamorphism. *Chemical Geology* **184**, 281–99.

LIATI A., GEBAUER D. & FANNING C. M. 2003. The youngest basic oceanic magmatism in the Alps (Late Cretaceous; Chiavenna unit, Central Alps): Geochronological constraints and geodynamic significance. *Contributions to Mineralogy and Petrology* **146**, 144–58.

LIATI A., GEBAUER D. & FANNING C. M. 2004. The age of ophiolitic rocks of the Hellenides (Vourinos, Pindos, Crete): First U–Pb ion microprobe (SHRIMP) zircon ages. *Chemical Geology* **207**, 171–88.

LIU S. F., STEEL R. & ZHANG G. W. 2005. Mesozoic sedimentary basin development and tectonic implication, northern Yangtze Block, eastern China: Record of continent–continent collision. *Journal of Asian Earth Sciences* **25**, 9–27.

LIU Z. W. 1994. Geochemistry of Precambrian volcanic rocks in Hunan and their tectonic setting. *Hunan Geology* **13** (3), 137–46 (in Chinese with English abstract).

LUDWIG K. R. 1999. *User's Manual for Isoplot/EX, Version 2.05, A Geochronolgical Toolkit for Microsoft Excel*. Berkeley Geochrono1ogica1 Center, Berkeley, CA (Special Publications, 1a).

LUDWIG K. R. 2001. *Squid 1.02: a User Manual*. Berkeley Geochronological Center, Berkeley, CA. (Special Publications, no. 2).

MANIKYAMBA C., KERRICH R., NAQVI S. M. & MOHAN M. R. 2004. Geochemical systematics of tholeiitic basalts from the 2.7 Ga Ramagiri-Hungund composite greenstone belt, Dharwar craton. *Precambrian Research* **134**, 21–39.

MEERT J. G. 2003. A synopsis of events related to the assembly of eastern Gondwana. *Tectonophysics* **362**, 1–40.

METCALFE I. 1996. Gondwanaland dispersion, Asian accretion and evolution of eastern Tethys. *Australian Journal of Earth Sciences* **43**, 605–23.

METCALFE I. 2000. Permian tectonic framework and Palaeogeography of SE Asia. *Journal of Asian Earth Sciences* **20**, 551–66.

METCALFE I., SHERGOLD I. H. & LI Z. X. 1993. IGCP 321 Gondwana dispersion and Asian accretion: Fieldwork on Hainan island. *Episodes* **16**, 443–7.

PEARCE J. A. & NORRY M. J. 1979. Petrogenetic implications of Ti, Zr, Y and Nb variations in volcanic rocks. *Contributions to Mineralogy and Petrology* **69**, 33–47.

PENG S. B., JIN Z. M., LIU Y. H. *et al.* 2006a. Petrochemistry, chronology and tectonic granitoids in Yunkai Orogenic Belt, setting of Strong Peraluminous Anatectic Western Guang Province, China. *Earth Science* **31** (**1**), 110–20 (in Chinese with English abstract).

PENG S. B., JIN Z. M., FU J. M., LIU Y. H., HE L. Q. & CAI M. H. 2006b. Geochemical characteristics of basic intrusive rocks in the Yunkai uplift Guangdong-Guangxi, China, and their tectonic significance. *Geological Bulletin of China* **25** (**4**), 434–41 (in Chinese with English abstract).

PILOT J., WERNER C. D., HAUBRUICH F. & BAUMANN N. 1998. Paleozoic and Proterozoic zircons from the Mid-Atlantic Ridge. *Nature* **393**, 676–9.

PIUZANA D., PIMENTEL M. M., FUCK R. A. & ARMSTRONG R. 2003. SHRIMP U-Pb and Sm-Nd data for the Araxá Group and associated magmatic rocks: Constraints for the age of sedimentation and geodynamic context of the southern Bras'lia Belt, central Brazil. *Precambrian Research* **125**, 139–60.

QIU Y. X., MA W. P., FAN X. L. *et al.* 1996. Tectonic nature and tectonic evolution of the 'Xuefeng Oldland' in the Caledonian stage. *Regional Geology of China* **19** (**2**), 150–60 (in Chinese with English abstract).

RAO J. R., WANG J. H. & CHAO Y. Z. 1993. Deep structure in Hunan province. *Hunan Geology* **7** (Suppl.), 1–100 (in Chinese).

REN S. L., LI J. L., ZHOU X. H. & SUN M. 1997a. Petrochemistry and mineral chemistry studies on metamorphic ultramafic rocks in Yanghou area, Zhenhe county, Fujian Province, China. *Geochimica* **26** (**4**), 13–23 (in Chinese with English abstract).

REN S. L., LI J. L., ZHOU X. H. & SUN M. 1997b. Study on geochronology and lithogeochemistry of the Xiongshan dyke swarm in northern Fujian, China. *Science in China (Series D)* **27** (**2**), 115–20 (in Chinese).

REVILLON S., ARNDT N. T., HALLOT E., KERR A. C. & TARNEY J. 1999. Petrogenesis of picrites from the Caribbean Plateau and the North Atlantic magmatic province. *Lithos* **49**, 1–21.

ROBERTSON A. H. F. 2002. Overview of the genesis and emplacement of Mesozoic ophiolites in the Eastern Mediterranean Tethyan region. *Lithos* **65** (**1–2**), 1–67.

RUBATTO D., GEBAUER D. & FANNING M. 1998. Jurassic formation and Eocene subduction of the Zermatt-Saas-Fee ophiolites: Implications for the geodynamic evolution of the Central and Western Alps. *Contributions to Mineralogy and Petrology* **132**, 269–87.

SCHALTEGGER U., GEBAUER D. & VON QUADT A. 2002. The mafic–ultramafic rock association of Loderio-Biasca (lower Pennine nappes, Ticino, Switzerland): Cambrian oceanic magmatism and its bearing on early Paleozoic paleogeography. *Chemical Geology* **186**, 265–79.

SCHMITT R. S., TROUW R. A. J., VAN SCHMUS W. R. & PIMENTEL M. M. 2004. Late amalgamation in the central part of West Gondwana: New geochronological data and the characterization of a Cambrian collisional orogeny in the Ribeira Belt (SE Brazil). *Precambrian Research* **133**, 29–61.

SCHULZ B., KLEMD R. & BRÄTZ H. 2006. Host rock compositional controls on zircon trace element signatures in metabasites from the Austroalpine basement. *Geochimica et Cosmochimica Acta* **70**, 697–710.

SHERVAIS J. W. 1982. Ti, V plot and the petrogenesis of modern and opholitic lavas. *Earth and Planetary Science Letters* **59**, 101–18.

SONG B., ZHANG Y. H. & WAN Y. S. 2002. Mount making and procedure of the SHRIMP dating. *Geological Review* **48** (Suppl.), 26–30 (in Chinese with English abstract).

SUN S.-S. & MCDONOUGH W. F. 1989. Chemical and isotopic systematics of oceanic basalt: Implication for mantle composition and processes. *In* Saunders A. D. & Norry M. J. (eds). *Magmatism in the Ocean Basins*, Special publications, **42** , pp. 528–48. Geological Society, London.

TANG X. S., HUANG J. Z. & GUO I. Q. 1997. Hunan Banxi Group and its tectonic environment. *Hunan Geology* **16** (4), 219–26 (in Chinese with English abstract).

TEKLAY M., KRÖNER A. & MEZGER K. 2002. Enrichment from plume interaction in the generation of Neoproterozoic arc rocks in northern Erit area: Implications for crustal accretion in the southern Arabian–Nubian Shield. *Chemical Geology* **184**, 167–84.

VAVRA G., GEBAUER D., SCHMID R. & COMPSTOM W. 1996. Multiple zircon growth and recrystallisation during polyphase Late Carboniferous to Triassic metamorphism in granulites of the Ivrea Zone (Southern Alps): An ion microprobe (SHRIMP) study. *Contributions to Mineralogy and Petrology* **122**, 337–58.

WANG J. H., TU X. L. & SUN D. Z. 1999. U-Pb dating of anatectic migmatites at Gaozhou in the Yunkai Block, western Guangdong, China. *Geochimica* **28** (**3**), 231–8 (in Chinese with English abstract).

WANG X. F., MA D. Q. & JIANG D. 1991. *Geology in Hainan Island*. Geological Publishing House, Beijing (in Chinese).

WILDE S. A., WU F. Y. & ZHANG X. Z. 2003. Late Pan-African magmatism in northeastern China: SHRIMP U-Pb zircon evidence from granitoids in the Jiamusi Massif. *Precambrian Research* **122**, 311–27.

WILLIAMS I. S. 1992. Some observations on the use of zircon U-Pb geochronology in the study of granite rocks. *Transactions of the Royal Society of Edinburgh-Earth Sciences* **83**, 447–58.

WU H. R. 2003. Tectono-Paleogeographic analysis of the geologic problems related to ophiolitic belt in Jiangxi Province. *Journal of Palaeogeography* **5** (3), 328–42 (in Chinese with English abstract).

XIA B. D., SHI G., FANG Z. *et al.* 1991a. The rift action in later Paleozoic era on Hainan Island. *Journal of Geology* **2**, 103–15 (in Chinese with English abstract).

XIA B. D., YU J. H., FANG Z., WANG C. Y. & SHI G. Y. 1991b. The Carboniferous bimodal volcanic rocks in Hainan Island and their plate tectonic setting. *Acta Petrologica Sinica* **1**, 55–62.

XU D. R., LIN G., LIANG X. Q., CHEN G. H. & TANG H. F. 2001. The records of the evolution of Precambrian lithosphere-the evidences of petrology and geochemistry of Basic rocks On Hainan Island. *Acta Petrologica Sinica* **17**, 589–609 (in Chinese with English abstract).

XU D. R., XIA B., NONNA B. C. *et al.* 2006. Metamorphic characteristics of the Chenxing metabasite massif in Tunchang area, Hainan Island, South China and its tectonic implication. *Acta Petrologica Sinica* **22** (**12**), 3987–3006 (in Chinese with English abstract).

XU D. R., NONNA B. C., ROBERT B. *et al.* 2007. The Tunchang area metabasites in the East-central Hainan Island, China: Geochemistry and Sr-Nd isotope systematics. *Mineralogy and Petrology* (in press).

YAN D. P., ZHOU M. F., SONG H. L., WANG X. W. & MALPAS J. 2003. Origin and tectonic significance of a Mesozoic multi-layer over-thrust system within the Yangtze Block (South China). *Tectonophysics* **361**, 39–254.

YANG S. F., YU Z. Y., GE L. Z. & SHI Y. S. 1989. Differentiation of Hainan terrane, the research of paleogeomagnetism and the significance of plate tectonics. *Journal of Nanjing University (Earth Science)* **1** (**1–2**), 38–46 (in Chinese with English abstract).

YANG S. F., CHEN H. L., WU G. H. & TONG Z. W. 1995. Distcovery of early Paleozoic island-arc volcanic rocks in northern part of Fujian Province and the significance for tectonic study. *Scientia Geologica Sinica* **30** (**2**), 106–16 (in Chinese with English abstract).

ZENG Q. L., YUAN C. L., GUO Z. M. & LIN J. M. 1992. *Fundamental Geological Investigation of Sanya, Hainan Island*. The Press of the China University of Geoscinences, Wuhan (in Chinese with English abstract).

ZHANG B. Y., ZHAO Z. H., SHI M. Q., YANG S. F. & CHEN H. L. 1997a. The confirmation of the Permian island arc basalt in Chenxi area and its tectonic significance: Implication for Paleo-Tethys tectonic zone in the boundary between Guangdong and Guangxi Provinces. *Chinese Science Bulletin* **42** (4), 413–16.

ZHANG Q., ZHOU D. J., ZHAO D. S. *et al.* 1994. Ophiolites of the Hengduan Mountains, China: Characteristics and tectonic settings. *Journal of Southeast Asian Earth Sciences* **9**, 335–44.

ZHANG Y. M., FU J. M., ZHAO Z. J., XU A., WU G. G. & ZENG B. 1997b. The Precambrian crustal tectonic evolution in Hainan Island. *Earth Science* **22**, 395–400 (in Chinese with English abstract).

ZHANG Y. M., ZHANG R. J., YAO H. & MA G. 1998. Petrographic characteristics and Sm-Nd isotopic dating of the metamorphic basic volcanic rocks in western part of Hainan island. *Journal of Mineralogy and Petrology* **1**, 78–84 (in Chinese with English abstract).

ZHANG Z. M., YOU Z. D., HAN Y. & SONG L. K. 1995. Petrology, metamorphic process and genesis of the Dabie-Sulu eclogite belt, east-Central China. *Acta Geologica Sinica* **69** (4), 306–25 (in Chinese with English abstract).